Journal of Medicinal Chemistry

Article

pubs.acs.org/jmc

8-Substituted O^6-Cyclohexylmethylguanine CDK2 Inhibitors: Using Structure-Based Inhibitor Design to Optimize an Alternative Binding Mode

Benoit Carbain,[⊥,‡] David J. Paterson,[⊥,†] Elizabeth Anscombe,[†] Allyson J. Campbell,[‡] Celine Cano,[‡] Aude Echalier,[†,▽] Jane A. Endicott,*[,†,#] Bernard T. Golding,[‡] Karen Haggerty,[‡] Ian R. Hardcastle,[‡] Philip J. Jewsbury,[§] David R. Newell,[∥] Martin E. M. Noble,[†,#] Celine Roche,[‡] Lan Z. Wang,[∥] and Roger J. Griffin*[,‡]

[†]Department of Biochemistry, University of Oxford, South Parks Road, Oxford OX1 3QU, U.K.

[‡]Newcastle Cancer Centre, Northern Institute for Cancer Research, School of Chemistry, Newcastle University, Bedson Building, Newcastle upon Tyne NE1 7RU, U.K.

[§]AstraZeneca Pharmaceuticals, Alderley Park, Cheshire SK10 4TG, U.K.

[∥]Newcastle Cancer Centre, Northern Institute for Cancer Research, Newcastle University, Paul O'Gorman Building, Medical School, Framlington Place, Newcastle upon Tyne NE2 4HH, U.K.

Supporting Information

ABSTRACT: Evaluation of the effects of purine *C*-8 substitution within a series of CDK1/2-selective O^6-cyclohexylmethylguanine derivatives revealed that potency decreases initially with increasing size of the alkyl substituent. Structural analysis showed that *C*-8 substitution is poorly tolerated, and to avoid unacceptable steric interactions, these compounds adopt novel binding modes. Thus, 2-amino-6-cyclohexylmethoxy-8-isopropyl-9*H*-purine adopts a "reverse" binding mode where the purine backbone has flipped 180°. This provided a novel lead chemotype from which we have designed more potent CDK2 inhibitors using, in the first instance, quantum mechanical energy calculations. Introduction of an *ortho*-tolyl or *ortho*-chlorophenyl group at the purine C-8 position restored the potency of these "reverse" binding mode inhibitors to that of the parent 2-amino-6-cyclohexylmethoxy-9*H*-purine. By contrast, the corresponding 8-(2-methyl-3-sulfamoylphenyl)-purine derivative exhibited submicromolar CDK2-inhibitory activity by virtue of engineered additional interactions with Asp86 and Lys89 in the reversed binding mode, as confirmed by X-ray crystallography.

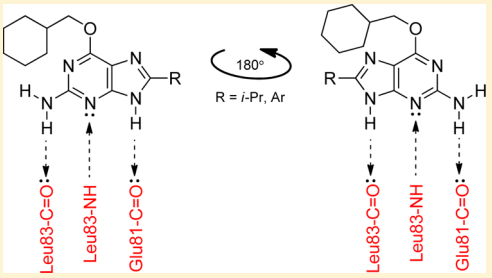

INTRODUCTION

Deregulation of the cell cycle is a vital motif in most, if not all, human malignancies.[1,2] Phosphorylation of pRb, the product of the retinoblastoma gene, by cyclin-dependent kinase (CDK) family members, is required for G1 progression, and mutation of the pRb gene or abnormalities in the pRb signaling pathway are a common feature of cancer. For example, overexpression and/or mutation of CDK4 and cyclin D has been reported in various tumor types, and mutation of the $p16^{INK4A}$ gene that results in its deletion or silencing is one of the most frequent genetic alterations found in human tumors.[3,4] Overexpression of cyclin E and reduced levels of $p27^{Kip1}$ have also been observed to correlate with disease progression,[5,6] suggesting that deregulation at various checkpoints throughout the cell cycle is a key contributor to the process of tumorigenesis. As a result of these studies, the CDK family is considered an important target for therapeutic intervention in cancer and other diseases, and a wide range of ATP-competitive inhibitors have been developed.[7−9] However, although a number of small-molecule CDK inhibitors have progressed to clinical trials (e.g., **1**−**4**), a kinase-specific CDK inhibitor has yet to be approved by the FDA for clinical use.[7,10,11]

Initial enthusiasm for CDK2 as a cancer therapeutic target was tempered by subsequent studies demonstrating that CDK2 siRNA or antisense constructs failed to induce cell cycle arrest in a number of human tumor cell lines[12] and that CDK2 knockout mice are viable.[13,14] However, more recent evidence suggests that CDK2 inhibition may elicit antitumor activity in a subset of tumors with defined genetic characteristics. For example, CDK2 knockdown or treatment with roscovitine (**1**) is selectively toxic to *MYCN*-amplified neuroblastoma cells compared with their nonamplified counterparts.[15] Compelling evidence to support a therapeutic role for pharmacological CDK2 inhibition in cancer treatment has also been adduced very recently by employing a chemical genetic approach.[16] Thus, a comparison of selective small-molecule CDK2 inhibition with that imposed by siRNA knockdown in normal and tumor cells highlighted important

Received: August 20, 2013

   dx.doi.org/10.1021/jm401555v | *J. Med. Chem.* XXXX, XXX, XXX−XXX

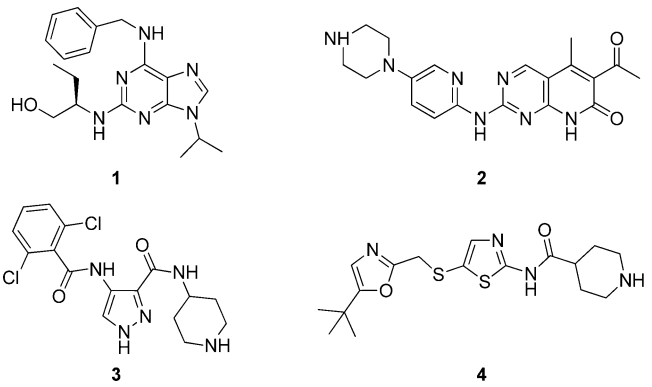

differences between these approaches, with pharmacological inhibition resulting in growth inhibition of a panel of human cancer cells transformed with various oncogenes. A recent study demonstrating that a combination of phosphatidylinositol-3-kinase (PI3-K) and CDK2 inhibitors induced apoptosis in malignant glioma xenografts via a synthetic−lethal interaction also highlights the potential of CDK2-selective inhibitors.[17]

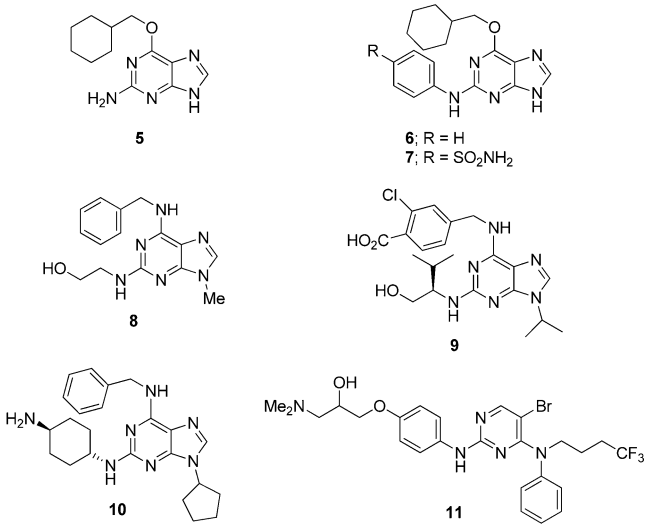

We have previously reported the structure-based design of a series of potent CDK2-selective inhibitors derived from the lead compound O^6-cyclohexylmethylguanine (NU2058, **5**; CDK2 IC_{50} = 16.0 μM), as exemplified by **6** and **7** (CDK2; IC_{50} = 1.0 μM and 5.0 nM, respectively).[18−22] The X-ray crystal structure of **5** in complex with monomeric unphosphorylated CDK2 revealed that the purine heterocycle binds within the ATP-binding pocket in a different orientation from that previously reported for ATP, isopentenyladenine, and the prototypic purine CDK inhibitor olomoucine (**8**).[23] The 9-NH group of **5** forms a hydrogen-bond with the backbone carbonyl of Glu81, while the purine *N*-3 and 2-amino group make hydrogen bonds with the backbone nitrogen NH and carbonyl of Leu83, respectively. In this orientation, the C-8 position of **5** is directed toward the side-chain of Phe80 in the gatekeeper pocket (Figure 1). A number of purine-based CDK inhibitors derive potency from interacting with this residue; for example, purvalanol B (**9**)[24] and H717 (**10**)[25] both pack hydrophobic aliphatic substituents against the Phe80 side chain. In contrast, a series of bisanilinopyrimidines (e.g., **11**) abut polar and polarizable groups against the phenyl ring of Phe80, and the observed gain in potency for this compound series is attributed to induced dipole−dipole interactions.[26,27]

The close proximity of the imidazole ring of **5** to the Phe80 side chain observed in the structure of the inhibitor in complex with CDK2 implied that substitution at the purine C-8 position would not be tolerated. To confirm this prediction, and as part of SAR studies for this chemotype, three derivatives of **5** bearing alkyl groups at the 8-position (**24**−**26**) were initially synthesized, and the crystal structure of the 8-isopropylpurine (**26**) bound to CDK2 was determined. Purine **26** was found to adopt a different binding orientation from that observed for **5** within the ATP-binding domain, offering the opportunity to exploit alternative inhibitor−protein interactions through judicious structural modifications to the parent purine **5**. In this paper, we describe the elaboration of this binding mode through iterative compound synthesis, molecular modeling, and X-ray crystallographic analysis of CDK2/cyclin A/inhibitor complexes. These studies have achieved improved CDK2-inhibitory activity by virtue of an engineered additional CDK2−inhibitor interaction.

CHEMISTRY

The initial target 8-substituted O^6-cyclohexylmethylguanine derivatives (**24**−**29**, **32**) were readily synthesized following the procedures illustrated in Scheme 1. Thus, acylation of the 6-amino group of 2,6-diamino-4-cyclohexylmethoxy-5-nitrosopyrimidine (**17**)[18] afforded the 6-acylaminopyrimidines (**18**-**23**), which were readily cyclized to the required purines (**24**−**29**) in good overall yields on reduction of the 5-nitroso substituent by catalytic hydrogenation. Efforts to prepare the 8-trifluoromethylpurine **32** by this approach were unsuccessful, with **17** proving refractory to

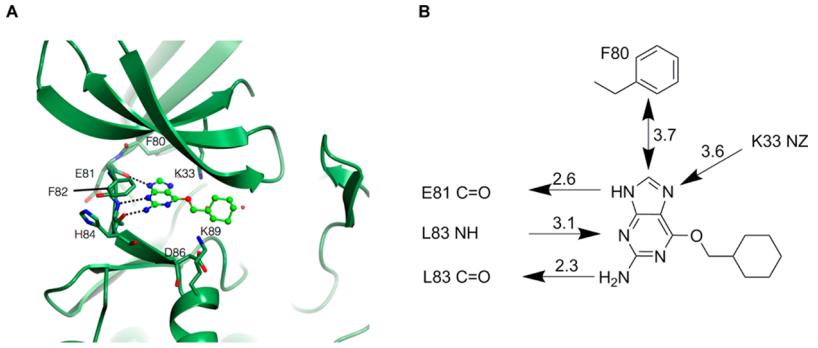

Figure 1. (A) Purine **5** bound to the CDK2 ATP-binding domain. The kinase is presented in dark green in ribbon representation, and selected CDK2 residues and **5** are drawn in ball-and-stick mode. Carbon atoms of **5** are colored light green, and hydrogen bonds are denoted by dashed lines. (B) Schematic representation of the bonds made between CDK2 and **5**. Hydrogen bonds are drawn as arrows. The double-headed arrow denotes the distance (Å) between the purine C8 atom and the side-chain of Phe80.

dx.doi.org/10.1021/jm401555v | *J. Med. Chem.* XXXX, XXX, XXX−XXX

Scheme 1[a]

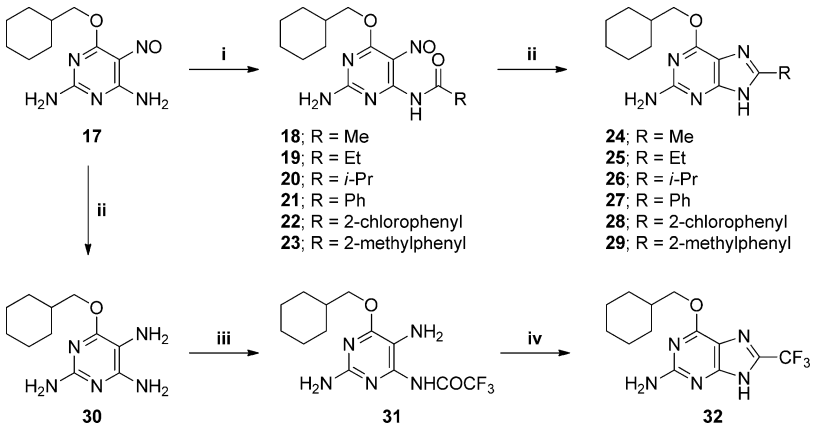

[a]Reagents and conditions: (i) **18**–**21**, $(RCO)_2O$, DMF, 80 °C, **22** and **23**, ArCOCl, pyridine, DMAP, 25 °C; (ii) H_2, Pd/C, AcOH, THF, 20 °C; (iii) TFA, reflux; (iv) DMAP, pyridine, reflux.

Scheme 2[a]

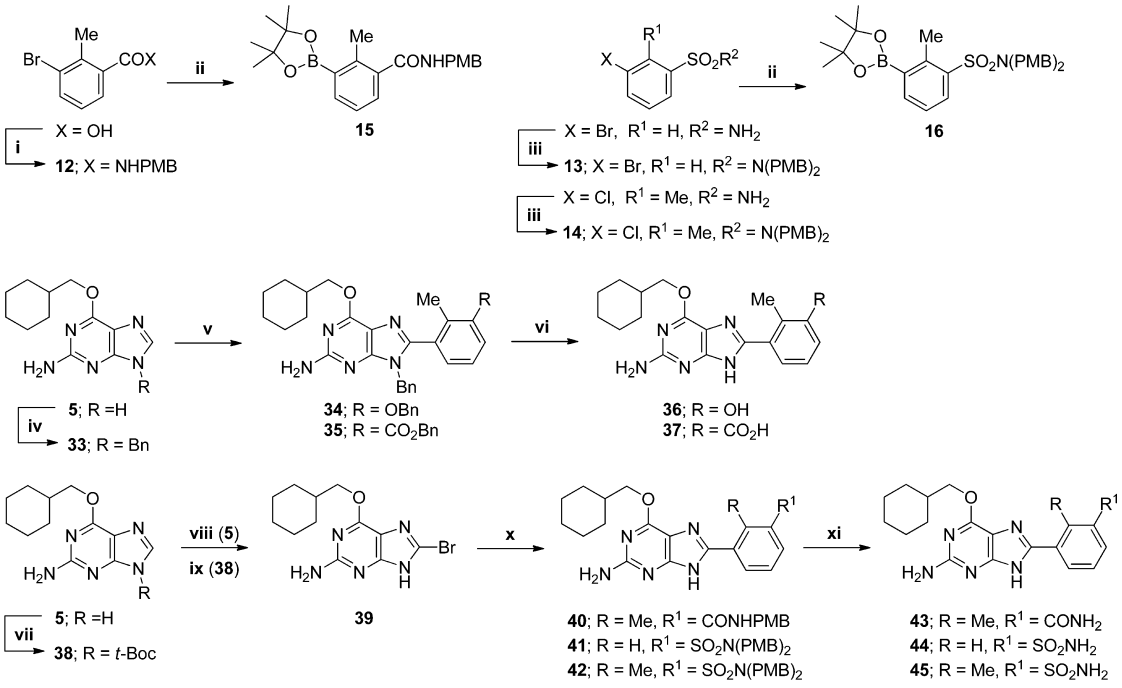

[a]Reagents and conditions: (i) (a) TsCl, pyridine, 0–25 °C, (b) PMB-Cl, DMAP, 25 °C; (ii) bis(pinacolato)diboron, $PdCl_2[[(C_4H_9)_2PC_5H_4]_2Fe]$, $[(C_4H_9)_2PC_5H_4]_2Fe$, KOAc, dioxane, MW 150 °C; (iii) PMB-Cl, NaH, DMF, 80 °C (**13**) 25 °C (**14**); (iv) BnBr, K_2CO_3, DMF, 25 °C; (v) $Pd(OAc)_2$, CuI, $CsCO_3$, DMF, MW 200 °C; (vi) H_2, Pd/C, AcOH, aq. HCl, 20 °C; (vii) $(tBuO)_2CO$, K_2CO_3, DMF, 20 °C; (viii) pyridinium tribromide, DCM, 70 °C; (ix) NBS, MeCN, 20 °C; (x) appropriate arylboronate, $PdCl_2[[(C_4H_9)_2PC_5H_4]_2Fe]$, Cs_2CO_3, aq dioxane, 110 °C; (xi) TFA, 20–110 °C.

acylation with TFA-anhydride or ethyl trifluoroacetate. However, direct acylation of triaminopyrimidine **30** with TFA gave the required trifluoroacetylaminopyrimidine **31**, which slowly cyclized to the requisite purine **32** on prolonged heating in pyridine-DMAP.

The preparation of O^6-cyclohexylmethylguanine derivatives bearing substituted aryl groups at the purine 8-position required palladium-catalyzed cross-coupling methodology (Scheme 2). Direct 8-arylation of the N^9-benzylpurine **33** with the appropriate aryl bromides, employing CuI–$Pd(OAc)_2$ under microwave irradiation, furnished benzyl-protected intermediates **34** and **35**, and subsequent conversion into the requisite phenol **36** and benzoic acid **37** was achieved in moderate yield by catalytic hydrogenation under acidic conditions. An alternative approach utilized the 8-bromopurine **39**, readily synthesized by treatment of the *t*-BOC-protected purine derivative **38** with *N*-bromosuccinimide, which concomitantly removed the protecting group, or via direct bromination of **5** with pyridinium tribromide. Suzuki–Miyaura cross coupling of **39** with the appropriate boronate derivatives (**15**, **16**), prepared from the corresponding aryl halides (**12**, **14**) by standard methods, or generated in situ from **13**, gave the PMB-protected compounds (**40**–**42**), which were smoothly deprotected to the required 8-substituted purines **43**–**45** on treatment with TFA.

dx.doi.org/10.1021/jm401555v | J. Med. Chem. XXXX, XXX, XXX–XXX

Table 1. Inhibition of CDK1 and CDK2 by C8-Substituted O^6-Cyclohexylmethylguanines

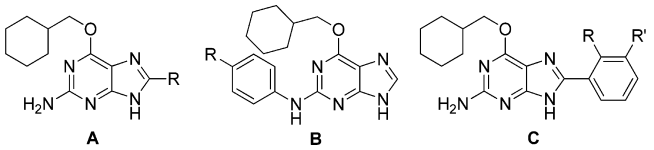

				IC_{50} (μM)[a] or % inhibition	
no.	structure	R	R′	CDK2/cyclin A	CDK1/cyclin B
5	A	H		16 ± 2.0[b]	26 ± 3.5
6	B	H		0.97 ± 0.03	10.0 ± 1.6
7	B	SO_2NH_2		0.005 ± 0.001	0.25 ± 0.05
24	A	Me		44.7 ± 3.2	7%, 11%[c]
25	A	Et		30.3 ± 1.5	77.5
26	A	*i*-Pr		27.7 ± 3.2	92.3 ± 4.3
27	C	H	H	10%[c]	35%[c]
28	C	Cl	H	17 ± 1.8	>100
29	C	Me	H	18.2 ± 4.3	93.6[d]
32	A	CF_3		49 ± 2.6[e]%	>100
36	C	Me	OH	23.5 ± 4.8	>100
37	C	Me	CO_2H	>100	>100
43	C	Me	$CONH_2$	39.8 ± 13.9	62%[d]
44	C	H	SO_2NH_2	8.7 ± 3.4	>100
45	C	Me	SO_2NH_2	0.51 ± 0.05	2.8[d]

[a]IC_{50} values determined as described in ref 20. [b]Standard deviations obtained from three separate experiments. [c]Activity determined at 10 μM owing to limiting solubility. [d]Single determination. [e]Activity measured at 100 μM.

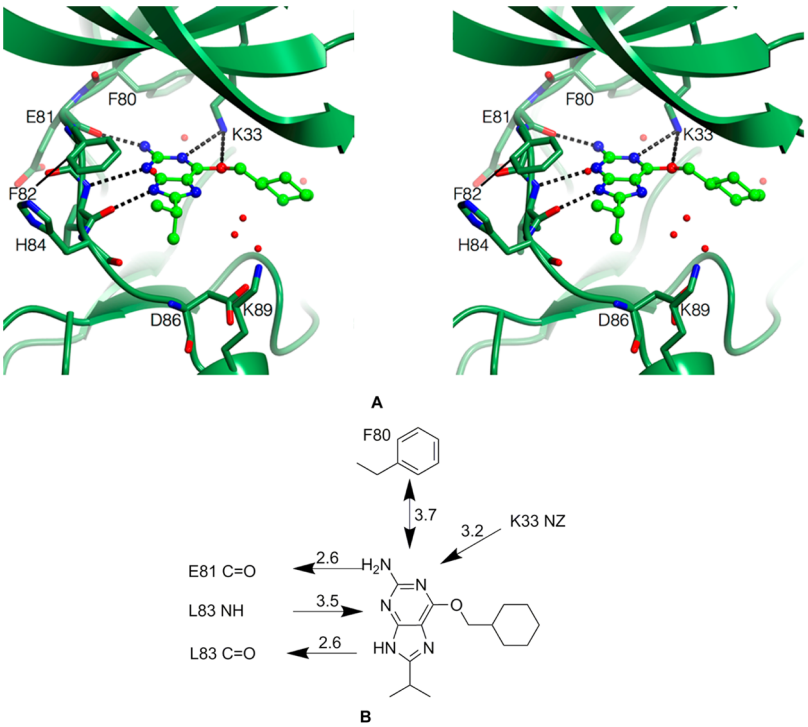

Figure 2. (A) Stereoview of **26** in complex with CDK2. The kinase is presented in dark green in ribbon representation, and selected CDK2 residues and **26** are drawn in ball-and-stick mode. Carbon atoms of **26** are colored light green, and hydrogen bonds are denoted by dashed lines. Water molecules are drawn as red spheres. (B) Schematic representation of the bonds made between CDK2 and **26**. Hydrogen bonds are drawn as arrows. The double-headed arrow denotes the distance (Å) between the purine C2 substituent and the side chain of Phe80.

RESULTS AND DISCUSSION

The inhibitory activity of the purine derivatives against CDK1 and CDK2 is shown in Table 1. Our previous studies with O^6-alkylguanines were founded on the benchmark O^6-alkylguanine NU2058 (**5**) and culminated in the identification of NU6102 (**7**), a highly selective CDK2 inhibitor that was developed by a structure-based inhibitor design approach. The markedly increased potency of **7** (CDK2; IC_{50} = 5 nM) compared with **5** (CDK2; IC_{50} = 16 μM) is attributed to additional favorable interactions between the sulfonamide function of **7** and the specificity surface of the ATP-binding domain of the kinase.[20] The

dx.doi.org/10.1021/jm401555v | J. Med. Chem. XXXX, XXX, XXX−XXX

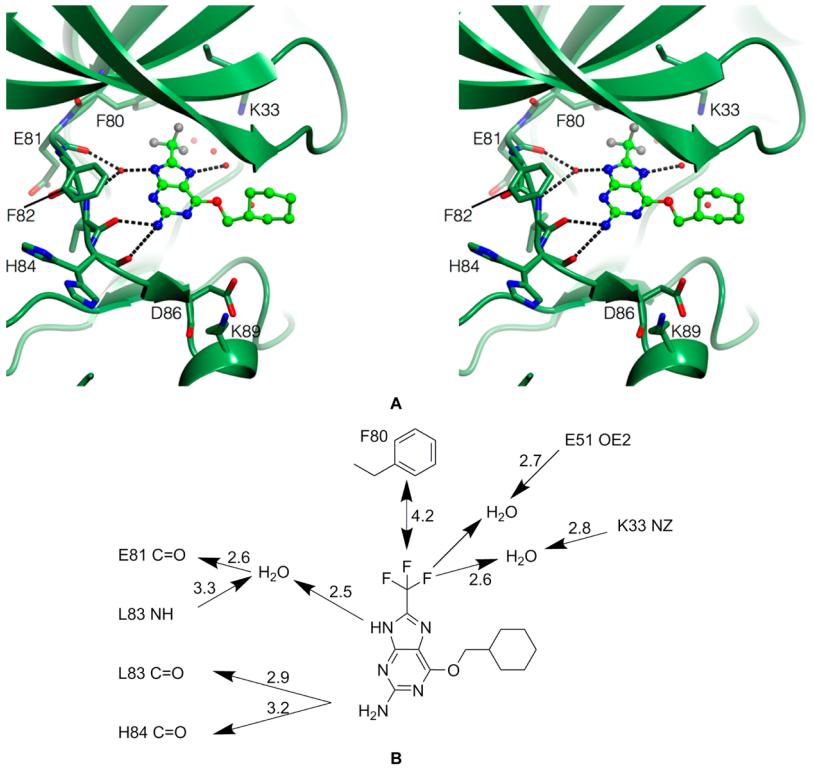

Figure 3. (A) Stereoview of **32** in complex with CDK2/cyclin A. The kinase is presented in dark green in ribbon representation, with selected CDK2 residues and **32** drawn in ball-and-stick mode. Carbon atoms of **32** are colored light green, and hydrogen bonds are denoted by dashed lines. Water molecules are drawn as red spheres. (B) Schematic representation of the bonds made between CDK2 and **32**. Hydrogen bonds and polar interactions are drawn as arrows. The double-headed arrow denotes a potential hydrophobic interaction between the purine C8 substituent and the side chain of Phe80.

primary sulfonamide function of **7** also provided an opportunity to develop a water-soluble prodrug, by virtue of *N*-acetylation and formulation as the potassium salt, and in vivo studies are in progress.[28] With a view to further delineating SARs for this interesting class of kinase inhibitor, the effect of substitution at the C-8 position of **5** was investigated.

The crystal structure of **5** bound to CDK2/cyclin A indicated that 8-substitution would not be well tolerated, as a result of a steric clash between the C-8 moiety and the side-chain of Phe80 ($r_{C8-F80C\beta}$ = 3.7 Å in the CDK2/**5** structure).[20] This observation appeared to be confirmed by the CDK2-inhibitory activity of the three initial derivatives, which showed a modest decrease in potency compared with **5** on addition of a methyl (**24**), ethyl, (**25**), or isopropyl (**26**) group at the purine 8-position (IC_{50} values of 45, 30, and 28 μM, respectively), albeit that **25** and **26** were essentially equipotent with **24** despite steric differences (Table 1). Where measurable, activity against CDK1 compared with CDK2 also generally tracked that observed for **5**, with **25** and **26** proving some 2−3 times less potent against CDK1. Notably, a dramatic reduction in potency against both kinases was observed upon introduction of the bulky C-8 phenyl group, although a precise determination of the activity of **27** was limited by very poor aqueous solubility.

Crystal Structure Analysis. To establish the binding mode of this inhibitor series within the ATP pocket, X-ray crystallographic analysis of the 8-isopropyl- and 8-trifluoromethyl-purines (**26** and **32**) in complex with CDK2 was undertaken by following crystal soaking with each inhibitor. Interestingly, **26** was found to adopt a novel orientation within the ATP-binding site distinct from that observed for the parent CDK2 inhibitor **5** (Figure 2). By comparison with the "conventional" binding mode of **5** (Figure 1), the new orientation adopted by **26** can be described by a 180° rotation of the purine ring about a vector coincident with the C-6 to N-3 bond. In this orientation, C-8 of **26** is directed toward the "selectivity surface" of the kinase,[20,29] with the purine 2-amino group being projected toward Phe80. Thus, both **5** and **26** form a conserved triplet of hydrogen bonds with the CDK2 hinge region and the O^6-cyclohexylmethyl substituent is retained in the ATP ribose-binding pocket. In both cases, the conformation and location of the O^6-cyclohexylmethyl group is analogous to that previously observed for the structure of **7** bound to CDK2/cyclin A[20] (Supporting Information Figure S1).

Additional interactions of **26** with the glycine-rich loop of CDK2 contribute to stabilization of the activation segment, as previously observed for the structure of **5** bound to CDK2.[18] These interactions are predominantly lipophilic in nature, arising between the O^6-cyclohexyl ring of **5** and **26** and a hydrophobic patch on the glycine loop contributed by the side chain of residue Val18 and the peptide backbone around residue Gly11. The binding conformation adopted by **26** has not been reported previously despite extensive structural analyses of various substituted purine-based CDK ATP-competitive ligands.[18−20,22−24,30,31]

To assess whether smaller C-8 substituents would also promote this "reverse" binding mode, the 8-trifluoromethylpurine **32** was cocrystallized with CDK2/cyclin A phosphorylated on CDK2 Thr160 (CDK2/cyclin A). Previous comparative crystallographic studies of inhibitor binding to CDK2 and to CDK2/cyclin A have shown that the interactions made between inhibitors within this series, and the two alternative forms of CDK2 within the adenine binding pocket, are conserved. Surprisingly, **32** did not share the same binding mode as **26**, but rather adopted another that is

dx.doi.org/10.1021/jm401555v | *J. Med. Chem.* XXXX, XXX, XXX−XXX

reminiscent of, but distinct from, that of **5** (Figure 3). In contrast to the 8-isopropyl group of **26**, the 8-trifluoromethyl substituent of **32** was better accommodated, although this group is regarded as having a similar size to isopropyl.[32] The purine of **32** was found to bind in a near identical orientation to that of **5**, albeit less deeply within the CDK2 ATP-binding pocket. As a consequence, both the structure of the glycine-rich loop and the nature of the hydrogen bond interactions between **32** and the residues within the CDK2 hinge are modified. Most notably, the characteristic hydrogen bond interaction between the purine 9-NH and the backbone carbonyl moiety of Glu81 observed for **5** and **7** was absent with **32**. N-2 is positioned to enable hydrogen bonding with the carbonyl group of Leu83 or, for this inhibitor series, to form a novel interaction with the backbone carbonyl of His84. The 9-NH of **32** forms two indirect hydrogen bonds with CDK2 via a water molecule, which is also engaged in a polar contact with one of the fluorine atoms of the C-8 trifluoromethyl group that is packed against the Phe80 aromatic ring ($r(CF_3$-aromF80) = 4.2 Å). A second fluorine atom mediates a network of polar contacts with two water molecules that in turn interact with the side chains of Glu51 and Lys33 and the amide group of Asp145.

The CDK-inhibitory activity (Table 1) of the C-8 substituted purines (**24**–**27**, **32**) was reassessed in light of the structural biology results described above. The changes in potency observed against both CDK1 and CDK2 that accompany C-8 alkyl substitution, compared with the parent purine **5**, can be modeled as occurring in two phases as the size of the alkyl substituent increases. First, the initial decrease in potency is consistent with the formation of suboptimal interactions imposed to accommodate small alkyl groups such as methyl (**24**) at the purine C8 position. As illustrated by the structure of **32** in complex with CDK2/cyclin A (Figure 3), the inhibitor is forced away from Phe80 and, consequently, the requisite triplet of hydrogen bonds with the hinge cannot be maintained. Further small adjustments of the ATP site residues are also necessary to accommodate the inhibitor, and taken together, these changes lead to a decrease in binding affinity compared with **5** as reflected by CDK1/CDK2 inhibitory activity in the 100 μM range for **32**. Increasing the size of the C-8 substituent further results in an unacceptable steric clash with Phe80, and the inhibitor is forced to adopt an alternative binding mode where the C-8 group faces the selectivity surface, as observed with **26** (Figure 2).

Replicating the N-2 Aryl Group Interactions of 6 and 7 with CDK2 for C-8 Substituted Purines. The unique binding orientation adopted by the 8-isopropylpurine (**26**) offered an opportunity to design novel CDK2 inhibitors based on the 6-alkoxypurine template. Accordingly, we sought to exploit this finding by applying the structure-aided design principles employed previously for the optimization of the 2-arylaminopurines **6** and **7**[20] for the identification of more potent derivatives of **26**. A key feature of the binding of **6** and **7** to CDK2 is the packing of the N-2 aryl ring against the CDK2 surface to form a π–π stacking interaction with the peptide backbone between Gln85 and Asp86.[20] Notably, the aryl ring appears to have a low barrier to rotation about the N-2 to C-1′ bond, as demonstrated by the different purine–aryl interplane torsion angles of these and other derivatives.[20,22]

A structural superposition of **7** and **26** in complex with CDK2 and CDK2/cyclin A,[20] respectively (Supporting Information Figure S1), indicated that to replicate the aryl–backbone interactions made between **7** and CDK2, the aryl ring would need to be attached directly to the C-8 position, a compound that is most closely modeled in this series by the 8-phenylpurine **27**. However, the weak CDK2-inhibitory activity of **27** suggested that if, as predicted, the compound binds to CDK2 in the reverse binding mode, the requisite additional interactions are not arising between the 8-phenyl ring and the kinase. One possible explanation for this observation is that the purine and phenyl rings of **27** are essentially coplanar as a consequence of a favorable interaction of their π-systems, which would preclude the conformation necessary to facilitate an optimal interaction between the 8-phenyl ring and CDK2. Indeed, evidence in support of this is provided by the crystal structure of the aloisine derivative RP90 (6-phenyl[5*H*]pyrrolo[2,3-*b*]pyrazine) in complex with CDK2, where the pyrrole and 6-phenyl rings are found to adopt a coplanar conformation.[33]

With a view to optimizing the interaction of the 8-phenyl ring of **27** with the backbone of the ATP-binding domain of CDK2, the possibility of imposing a favorable conformational twist between the imidazole and phenyl rings, by virtue of *ortho*-substitution on the 8-phenyl ring, was considered. To this end, quantum mechanical calculations were employed to elucidate the conformation-energy profiles for nine derivatives of **27** to establish whether a noncoplanar conformation was energetically favorable, and to identify substituents with the potential to confer a nonplanar arrangement between the two ring systems. The ideal *ortho*-substituent on the 8-phenyl ring of **27** would induce an interplane twist of approximately 40°, with relatively free rotation arising about the optimum conformation of ±20°. This latter aspect would allow for optimization of aryl ring packing against the kinase. Such a twist was predicted to be tolerated based on literature evidence, where relatively large variations of torsion angles between nonconjugated ring systems have been observed for a number of purine-based inhibitors.[20,22,24]

Quantum Mechanical Calculations on Model Compounds Derived from 27. A simplified model of **27** was used to investigate the possibility of inducing a phenyl–purine twist with C-8 phenyl *ortho*-substituents. As a first approximation, it was assumed that the O^6-cyclohexylmethoxy substituent of **27** would have little effect on the phenyl–purine twist angle, and this group was not included in the calculations. Nine model compounds (**A**–**I**) encompassing combinations of fluoro, chloro, and methyl substituents were investigated in comparison with **27**. Each model was constructed and energy minimized, with the purine and aryl rings constrained to a coplanar orientation. A rigid potential energy scan was then performed at a range of interplanar angles between the two coplanar conformations (a full description of the results of this analysis for each compound can be found in the Supporting Information results and Figure S2).

The *ortho*-fluorophenylpurine (**A**) (Figure 4) was found to have both the desired characteristics of inducing an interplane twist of approximately 40° and allowing relatively free rotation about this optimum conformation. However, **A** possesses a significantly more stable conformation at 180°, presumably due to an intramolecular hydrogen bond. The 2-chlorophenyl derivative **B** has minima at approximately 40° and 140° that would, potentially, allow the formation of favorable aryl–backbone packing interactions. The 40° conformation is in a relatively shallow energy well, indicating some degree of rotation between the two ring systems. However, the more stable, and therefore preferred, conformation at 140° has a relatively steep energy well, implying a more restricted rotational freedom. By contrast, the *ortho*-methylphenylpurine **C** has a global minimum at around 40° in a relatively flat energy well. The *ortho*-disubstituted C8-phenylpurines **E**, **F**, **H**, and **I** all show potential to form the required conformation, especially the 8-(2-chloro-6-

dx.doi.org/10.1021/jm401555v | *J. Med. Chem.* XXXX, XXX, XXX–XXX

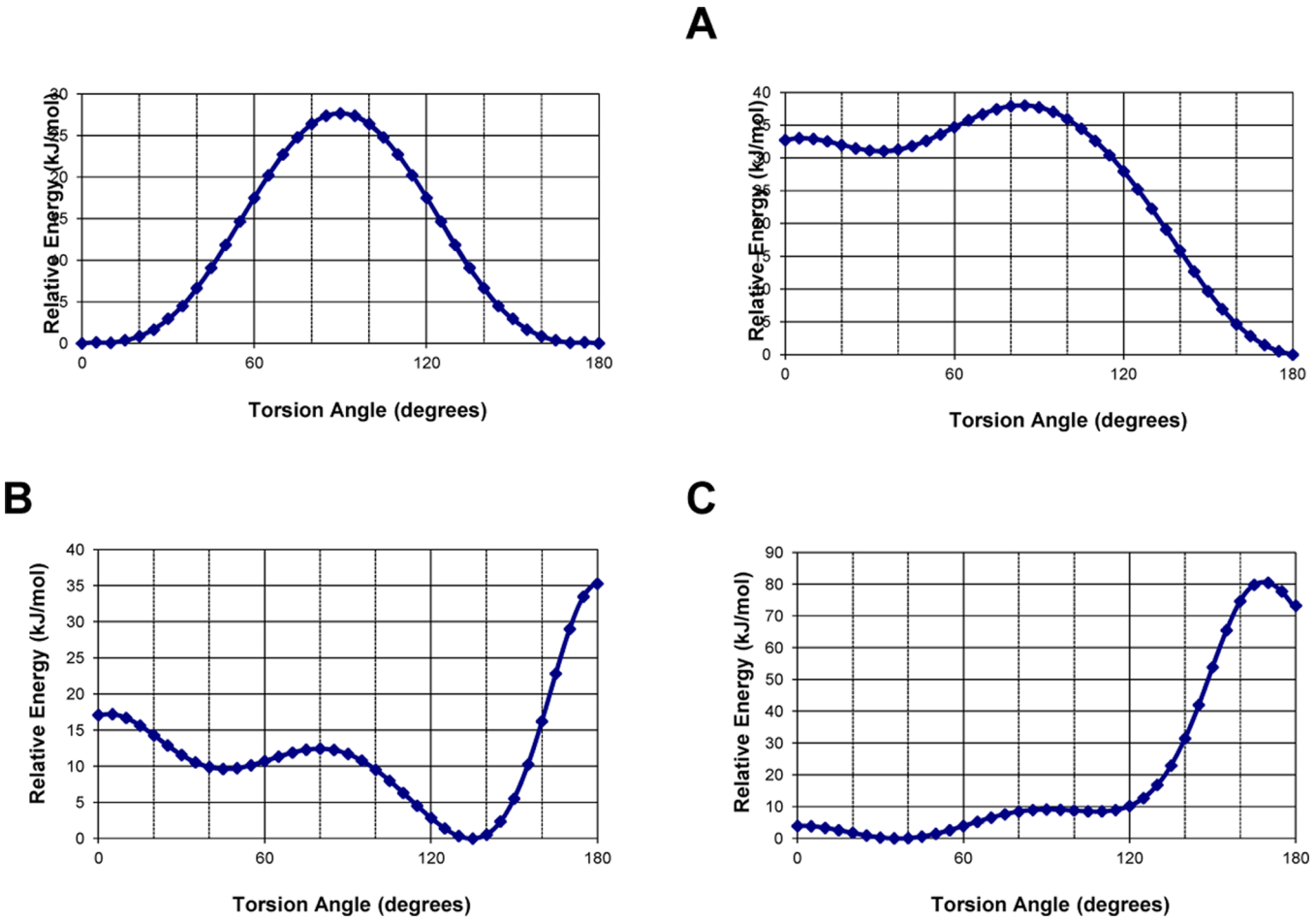

Figure 4. Conformation-energy profiles of **27** and three representative model compounds (A–C).

methylphenyl)purine (**I**), which has a minimum in a relatively flat energy well at ~50°.

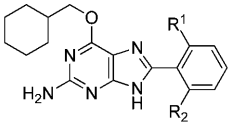

27; $R^1 = R^2 = H$ **D** ; $R^1 = R^2 = F$ **H** ; $R^1 = R^2 = Cl$
A ; $R^1 = F$, $R^2 = H$ **E** ; $R^1 = Me$, $R^2 = F$ **I** ; $R^1 = Me$, $R^2 = Cl$
B ; $R^1 = Cl$, $R^2 = H$ **F** ; $R^1 = Cl$, $R^2 = F$
C ; $R^1 = Me$, $R^2 = H$ **G** ; $R^1 = R^2 = Me$

To assess the validity of the modeling studies, the *ortho*-chlorophenyl and *ortho*-tolyl derivatives **B** and **C** were synthesized (**28** and **29**) and evaluated for CDK-inhibitory activity, with both compounds exhibiting potency comparable with the parent 2-amino-6-cyclohexylmethylpurine **5** (Table 1). Interestingly, **28** and **29** were essentially inactive against CDK1 (IC_{50} values of >100 and 94 μM, respectively), although the poor aqueous solubility of **27** militated against a direct comparison with **28** and **29**. The crystal structure of **29** in complex with CDK2/cyclin A was determined. As anticipated from the analysis of **26**, the *ortho*-tolylpurine **29** binds in the same reverse binding mode and makes an identical triplet of hydrogen bonds with Glu81 and Leu83 (Figure 5A). However, the interaction with Lys33 is not maintained, as the residue adopts a conformation in which the side chain is directed away from the inhibitor. The *o*-tolyl group of **29** is in the same orientation as the isopropyl group of **26** and projects toward the selectivity surface of the ATP pocket such that the C-8 atoms of compounds **26** and **29** almost coincide with the C-17 atom of **7** (first carbon atom of the 2-arylamino group, Figure 5B).

Importantly, the structure of **29** bound to CDK2/cyclin A supported the results of the quantum mechanical calculations. The *o*-tolyl group on the 8-aryl ring of the purine induces an inter-ring twist of approximately 38°, which is close to the predicted value of ~40°. This value is also similar to the inhibitor interplanar ring tilts observed for the CDK2/cyclin A/**6** and CDK2/cyclin A/**7** structures (50° and ~34°, respectively),[20] suggesting that an equivalent disposition of two-ring systems can be accommodated in either binding mode. The introduction of an *ortho*-methyl (or *ortho*-chloro) substituent onto the C-8 phenyl ring of **27** restores the potency of the compounds that adopt this altered binding mode to that of **5**, the benchmark 6-alkoxypurine CDK2 inhibitor in the series (Table 1). However, there remained a 20-fold difference in potency between **29** (CDK2; IC_{50} = 18.2 μM) and the 2-phenylaminopurine derivative **6** (CDK2; IC_{50} = 1.0 μM) that does not adopt the alternative binding mode. The lower potency of **29** likely results from misalignment of the purine, resulting in weakened hydrogen bond interactions with the CDK2 backbone in the hinge region. A concomitant shift of the purine ring out of the cleft will also result in suboptimal packing of the C-8 phenyl ring against the peptide backbone at residues Gln85 and Asp86.

Our previous studies with other purine- and pyrimidine-based CDK inhibitor series suggested the possibility of exploiting sequence differences between kinases on the "selectivity surface",

dx.doi.org/10.1021/jm401555v | *J. Med. Chem.* XXXX, XXX, XXX–XXX

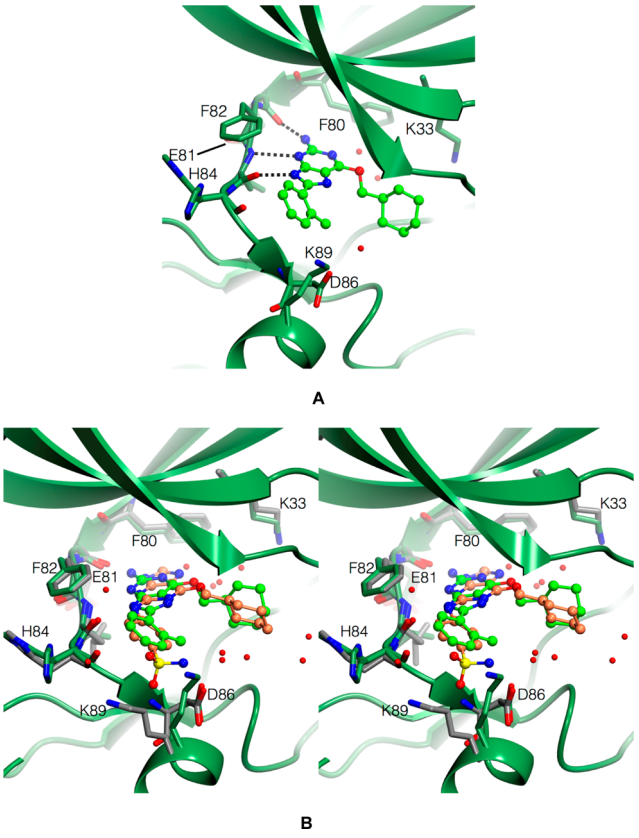

Figure 5. (A) Binding of **29** to CDK2/cyclin A. (B) Comparative binding of **7** and **29**. (A) CDK2 is shown in dark green. Selected residues from the CDK2 ATP binding pocket and **29** are shown as ball-and-stick representation and colored dark green and light green, respectively. Water molecules in the vicinity of the inhibitor are included as red spheres. (B) The inhibitors and selected residues within the CDK2 ATP binding site are shown in ball-and-stick representation. Carbon atoms of CDK2 residues from **7** and **29** complex structures are colored gray and dark green, respectively. Purine **7** is shown in coral and **29** in light green.

through further elaboration of the 8-aryl ring of **29**. For example, a number of inhibitor series probe both the conserved aspartate residue (Asp86 in CDK2) and the sequence differences that exist between CDKs at the residue equivalent to CDK2 Lys89 (Thr102 and Val100 in CDK4 and CDK7, respectively) to derive considerable gains in potency and selectivity.[20,24,26,34,35] The potent CDK2 inhibitor **7** evolved from **6** by the rational introduction of a sulfonamide group at the 4-position of the 2-phenylamino ring.[20] The resultant 200-fold increase in potency is attributable, at least in part, to optimal H-bond interactions arising between the sulfonamide moiety and the backbone amide and side chain of Asp86. In an effort to emulate these interactions in the context of the reversed binding mode, compound **29** was initially further substituted with hydroxyl (**36**) and carboxylate (**37**) groups at the *meta*-position on the C-8 aryl ring. However, these substitutions did not lead to a significant increase in potency, and while **36** (CDK2; IC_{50} = 28 μM) retained activity approaching that of **29** (CDK2; IC_{50} = 18.2 μM), the carboxylic acid derivative **37** was essentially devoid of activity against both CDK1 and CDK2 (IC_{50} > 100 μM). Determination of the structures of compounds **36** and **37** bound to CDK2/cyclin A revealed the molecular details of the inhibitor binding modes (Supporting Information Figure S3).

The disappointing activity of **36** and **37** prompted the introduction of *meta*-substituents on the 8-aryl ring having both donor and acceptor properties, with a view to recapitulating the interactions with Asp86 observed for **7**. Although the potency of the 3-carboxamido derivative **43** (CDK2; IC_{50} = 41/53 μM) suggested suboptimal binding, the introduction of a 3-sulfonamide group (**45**) conferred submicromolar CDK2-inhibitory activity (IC_{50} = 0.51 ± 0.05 μM). Thus, **45** proved approximately 50-fold more potent than **26** and exhibited activity comparable with the 2-phenylamino purine **6**. Interestingly, the 8-arylpurine **44**, which differs from **45** only in lacking the *ortho*-methyl group, was some 17-fold less potent (CDK2; IC_{50} = 8.7 ± 3.4 μM), supportive of the role of the *ortho*-methyl function in imposing the desired conformational twist of the 8-aryl ring of the purine.

The predicted binding modes of **44** and **45** were confirmed by determination of the structures of these purines bound to CDK2/cyclin A. Both inhibitors adopt the reverse binding mode, and, as predicted, the sulfonamide substituent makes hydrogen bonds to Asp86 and Lys89 (Figure 6). The presence of the 2-methyl group

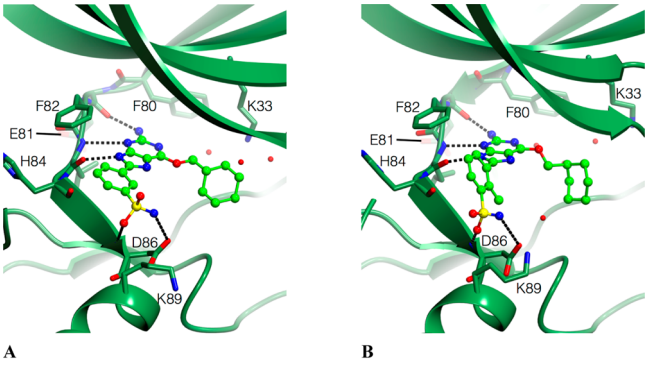

Figure 6. Crystal structures of (A) **44** and (B) **45** bound to CDK2/cyclin A. CDK2 is shown in green, with selected residues from the ATP-binding pocket shown in ball-and-stick mode. **44** and **45** are also drawn in ball-and-stick representation with carbon atoms colored light green.

on the C-8 aryl ring of **45** imposes the requisite rotation of the entire group and also precludes a steric clash between the methyl moiety and the N7 position. This rotation also results in a slight decrease in the distance between the sulfonamide substituent and Asp86 and Lys89 that may contribute to the observed increases in potency. The hydrogen bonds between the purine ring of **45** and the CDK2 backbone within the hinge sequence are maintained, but again a water molecule mediates an indirect network of interactions between N9 and the side chains of Lys33 and Glu81.

CONCLUSION

In the current study, the effect of substitutions at the C-8 position within a series of O^6-cyclohexylmethylguanines on their ability to inhibit CDK2 has been evaluated. The introduction of alkyl groups was poorly tolerated, leading to decreases in potency, the origins of which were elucidated by crystallographic analysis of selected inhibitors bound to CDK2/cyclin A. The crystal structures of compounds **26** and **32** bound to CDK2/cyclin A revealed that they adopt novel binding modes within the CDK2 ATP-binding site. An increase in the size of the C-8 alkyl group from methyl to isopropyl induced a rotation of the binding mode so that the C-8 substituent was positioned to face the CDK2 specificity surface. Quantum mechanical calculations were employed to identify **29**, a compound that adopts the novel, reverse binding mode and is equipotent with the parent purine **5** against CDK2.

dx.doi.org/10.1021/jm401555v | *J. Med. Chem.* XXXX, XXX, XXX–XXX

Initial further elaboration of **29** by *meta*-substitution to exploit potential interactions with Asp86 failed to increase potency. Structure determination of compounds **36** and **37** bound to CDK2/cyclin A revealed that these compounds occupy a similar position to compound **29** within the CDK2 ATP-binding cleft. However, despite interacting with the same region as the sulfonamide group of **7**, the hydroxyl and carboxylate substituents of **36** and **37**, respectively, are not oriented to reproduce the favorable interactions observed in the structure of **7**. However, in derivative **45**, a sulfonamide substituent at the *meta*-position of the C-8 arylpurine, in tandem with an *ortho*-methyl group, maintained the reversed binding mode and also emulated the interactions made by **7**, leading to the predicted increases in potency. Unfortunately, the relatively modest potency of **45** compared with the parent 2-arylamino-6-alkoxypurine CDK2 inhibitor **7**, combined with only limited opportunities for further elaboration, militate against further optimization of this series.

Small-molecule CDK inhibitors have enjoyed a resurgence of interest, as evidenced by a very recent review of the patent literature,[36] and clinical studies with the CDK4/6 inhibitor palbociclib (PD-0332991) are at an advanced stage.[37] These clinical studies are underpinned by a greater appreciation of the importance of CDK activity to normal cells, and the more careful selection of patient populations to ensure that effective therapeutic windows can be achieved. Previous experience has highlighted the importance of achieving selectivity for the target CDK over other family members, and the availability of crystal structures for the majority of the CDKs to guide inhibitor design, has proven invaluable. In this paper, we have demonstrated the application of molecular modeling and structure-based design for the exploitation of an unorthodox binding orientation of a purine-based CDK2 inhibitor. The results of the study contribute to a further understanding of the possible interactions of this inhibitor class with the ATP-binding domain of CDK2, and will be of value both in the design of more potent CDK2 inhibitors and for abrogating CDK2-inhibitory activity where this is required.

EXPERIMENTAL SECTION

General Synthetic Procedures. Reagents were purchased from fine chemicals vendors and used as received unless otherwise stated. Solvents were purified and stored according to standard procedures. Petrol refers to that fraction in the boiling range 40−60 °C. THF refers to anhydrous tetrahydrofuran, either by distillation from sodium benzophenone or from commercial sources. Melting points were obtained on a Stuart Scientific SMP3 apparatus and are uncorrected. Thin layer chromatography was performed using silica gel plates (Kieselgel 60F_{254}; 0.2 mm) and visualized with UV light or potassium permanganate. Chromatography was conducted under medium pressure in glass columns or using a Biotage SP4 instrument in prepacked columns (FLASH+ Silica columns [40−63 μm, 60 Å]). Semiprep HPLC was conducted with Varian ProStar HPLC system equipped with 2 ProStar 210 solvent delivery modules, a ProStar 320 UV−vis detector, a ProStar 701 fraction collector, and controlled by Varian Star chromatography workstation. Proton (^{1}H) and carbon (^{13}C) nuclear magnetic resonance (NMR) spectra were recorded on a Bruker Spectrospin AC 300E (^{1}H at 300 MHz, ^{13}C at 75 MHz), a Jeol JNM-LA500 spectrometer (^{1}H at 500 MHz, ^{13}C at 125 MHz), or a Bruker Avance II 500 (^{1}H at 500 MHz, ^{13}C at 125 MHz). Chemical shifts (δ) are reported in parts per million (ppm) downfield from tetramethylsilane (TMS), using known solvent peaks as internal standards. Coupling constants (J) are reported in hertz (Hz).

IR spectra were recorded on a Bio-Rad FTS 3000MX diamond ATR. Liquid chromatography−mass spectrometry (LCMS) was carried out on a Micromass Platform instrument operating in positive and negative ion electrospray mode, employing a 50 mm × 4.6 mm C18 column (Waters Symmetry or Waters Atlantis) 5 or 12 min gradient elution with 0.05% formic acid in methanol (10−90%). All compounds gave ≥95% purity by ^{1}H NMR, HPLC, or LCMS unless stated otherwise. Elemental analyses were performed by The School of Pharmacy, Analytical Facility, University of London, WC1N 1AX. Accurate masses were measured using a Finnigan MAR 95 XP or a Finnigan MAR 900 XLT at the EPSRC National Mass Spectrometry Service Centre (Chemistry Department, University of Wales, Swansea SA2 8PP, Wales).

*3-Bromo-N-(4-methoxybenzyl)-2-methylbenzamide (**12**).* *p*-Toluenesulfonyl chloride (1.06 g, 5.58 mmol) was added dropwise to a stirred solution of 3-bromo-2-methylbenzoic acid (1.0 g, 4.65 mmol) in anhydrous pyridine (5 mL) at 0 °C, and the mixture was allowed to warm to room temperature with stirring over 72 h. The solvent was removed in vacuo, and the residue was redissolved in EtOAc (20 mL), washed sequentially with aqueous HCl solution (0.1 M, 20 mL) and brine (2 × 20 mL), dried ($MgSO_4$), and concentrated under reduced pressure to give 3-bromo-2-methylbenzoic 4-methylbenzenesulfonic anhydride as a white solid (1.72 g, 100%), which was used directly for the next reaction. To a solution of the tosylate ester (0.46 g, 1.24 mmol) in DCM (5 mL) was added DMAP (15 mg, 0.12 mmol), and the mixture was stirred for 15 min at room temperature prior to addition of 4-methoxybenzylamine (0.8 mL, 6.3 mmol). After stirring for a further 30 min, DCM (10 mL) was added and the reaction mixture was washed sequentially with aqueous HCl solution (0.1 M, 20 mL) and brine (2 × 20 mL) and dried ($MgSO_4$), and the organic fraction was concentrated under reduced pressure. Purification by chromatography on silica, employing a gradient elution of petrol:EtOAc (9:1) to petrol:EtOAc (1:1), gave the title compound as a white powder (0.41 g, 100%); mp 121−122 °C. IR 3248, 1612, 1513 cm^{-1}. ^{1}H NMR ($CDCl_3$, 500 MHz) δ 2.44 (0.74H, s, Ar-CH_3), 2.47 (2.26H, s, Ar-CH_3), 3.78 (0.74H, s, OCH_3), 3.80 (2.26, s, OCH_3), 4.05 (0.49H, d, J = 6.1 Hz, NCH_2), 4.50 (0.25H, t, J = 5.9 Hz, NH), 4.55 (1.51H, d, J = 5.7 Hz, NCH_2), 5.95 (0.75H, br s, NH), 6.78−6.82 (0.48H, m, H-3′), 6.86−6.91 (1.51H, m, H-3′), 7.02−7.07 (0.75H, m, H-5), 7.08−7.13 (0.5H, m, H-2′), 7.25−7.29 (2.1H, m, H-4, H-2′), 7.31 (0.5H, d, J = 8.3 Hz), 7.58 (0.74H, dd, J = 8.0, 1.1 Hz, H-6), 7.73−7.77 (0.5H, m). ^{13}C NMR ($CDCl_3$, 125 MHz) δ 20.2, 21.7, 43.7, 46.9, 55.4, 55.5, 114.4, 114.2, 125.8, 126.8, 127.2, 127.3, 128.4, 129.4, 129.9, 130.0, 134.0, 135.7, 137.0, 138.8, 143.6, 159.5, 159.3, 169.2. HRMS [M + H]$^+$ ($C_{16}H_{17}BrNO_2$) calcd 334.0437, obsd 334.0438.

*3-Bromo-N,N-bis(4-methoxybenzyl)benzenesulfonamide (**13**).* NaH (60% in mineral oil, 75 mg; 1.86 mmol) was added to a solution of 3-bromobenzenesulfonamide (0.2 g, 0.85 mmol) in DMF (2 mL), and the solution was stirred at room temperature for 5 min. 4-Methoxybenzyl chloride (0.25 mL, 1.86 mmol) was added dropwise, and the mixture was stirred at 80 °C for 2 h and saturated aqueous ammonium chloride solution (5 mL). The resulting solution was extracted with DCM (3 × 20 mL), and the combined organic phases were dried ($MgSO_4$) and concentrated in vacuo. Purification by chromatography on silica, using a gradient elution of 100% EtOAc to petrol:EtOAc (5:1), gave the title compound as a crystalline white solid (0.34 g; 84%); mp 136−137 °C. IR 3009, 2837, 1608, 1509 cm^{-1}. ^{1}H NMR ($CDCl_3$, 500 MHz) δ 3.79 (6H, s, OCH_3), 4.27 (4H, s, NCH_2), 6.78 (4H, d, J = 8.6 Hz, H-3′), 7.01 (4H, d, J = 8.6 Hz, H-2′), 7.35 (1H, dd, J = 7.9, 8.0 Hz, H-5), 7.67 (1H, br d, J = 7.9 Hz, H-4), 7.72 (1H, br d, J = 7.9 Hz, H-6), 7.83 (1H, m, H-2). ^{13}C NMR ($CDCl_3$, 125 MHz) δ 49.8, 55.4, 114.0, 125.7, 127.3, 130.0, 130.1, 130.6, 135.4, 159.3. HRMS [M + H]$^+$ ($C_{22}H_{23}BrNO_4S$) calcd 476.0526, obsd 476.0522.

*3-Chloro-N,N-bis(4-methoxybenzyl)-2-methylbenzenesulfonamide (**14**).* To a solution of 3-chloro-2-methylbenzenesulfonamide (0.8 g, 3.89 mmol) in DMF (5 mL) was added NaH (60% in mineral oil, 0.2 g, 8.56 mmol), followed by 4-methoxybenzyl chloride (1.16 mL, 8.56 mmol). After stirring at room temperature for 1 h, saturated aqueous NH_4Cl solution (5 mL) was added to the reaction mixture, followed by H_2O (10 mL). The resulting solution was extracted with EtOAc (3 × 20 mL), and the combined organic fractions were washed with brine and dried ($MgSO_4$), and the solvent was removed in vacuo. Purification by chromatography on silica using gradient elution of 100% petrol to 30% petrol:EtOAc (3:1) afforded the benzenesulfonamide as a colorless crystalline solid (1.52 g, 88%); mp 66−68 °C. IR 2838, 1611, 1511 cm^{-1}. ^{1}H NMR ($CDCl_3$, 500 MHz) δ 2.63 (3H, s, Ar-CH_3), 3.80 (6H, s, OCH_3), 4.25 (4H, s, NCH_2), 6.81 (4H, d, J = 8.6 Hz, H-3′), 6.96 (4H, d, J

dx.doi.org/10.1021/jm401555v | J. Med. Chem. XXXX, XXX, XXX−XXX

= 8.6 Hz, *H*-2′), 7.23 (1H, dd, *J* = 7.9, 8.0 Hz, *H*-5), 7.59 (1H, dd, *J* = 8.0, 1.0 Hz, *H*-4), 7.89 (1H, dd, *J* = 7.9, 1.1 Hz, *H*-6). ^{13}C NMR (500 MHz,$CDCl_3$) 17.0, 48.8, 55.4, 114.1, 126.6, 127.2, 128.8, 130.2, 133.6, 135.9, 137.2, 140.9, 159.4. HRMS $[M]^+$ ($C_{23}H_{24}ClNO_4S$) calcd 445.1108, obsd 445.1109.

*N-(4-Methoxybenzyl)-2-methyl-3-(4,4,5,5-tetramethyl-1,3,2-dioxaborolan-2-yl)benzamide (**15**).* A mixture of **12** (0.16 mg, 0.49 mmol), bis(pinacolato)diboron (0.19 g, 0.74 mmol), [1,1′-bis-(diphenylphosphino)ferrocene]dichloropalladium(II) (17 mg, 0.024 mmol), 1,1′-bis(diphenylphosphino)ferrocene (26 mg, 0.048 mmol), and KOAc (0.144 g, 1.47 mmol) in dioxane (2 mL) was purged with N_2 and heated under microwave irradiation at 150 °C for 90 min. After cooling, the reaction mixture was filtered through Celite, EtOAc (10 mL) was added, and the mixture was washed with brine (2 × 10 mL) and dried ($MgSO_4$), and the solvents were evaporated under reduced pressure. Purification by chromatography on silica, employing a gradient eluent of petrol:EtOAc (10:1) to petrol:EtOAc (1:1), yielded the title compound as a colorless syrup (0.144 g, 77%). IR 3484, 3181, 2980, 2933, 1644, 1612, 1580, 1512 cm^{-1}. ^{1}H NMR ($CDCl_3$, 500 MHz) δ 1.34 (12H, s, CH_3), 2.44 (0.6H, s, Ar-CH_3), 2.60 (2.4H, s, Ar-CH_3), 3.78 (0.6H, s, OCH_3), 3.80 (2.4H, s, OCH_3), 4.05 (0.4H, d, *J* = 6.1 Hz, NCH_2), 4.51 (0.2H, t, *J* = 5.9 Hz, N*H*), 4.56 (1.6H, d, *J* = 5.6 Hz, NCH_2), 5.88 (0.8H, t, *J* = 4.9 Hz, N*H*), 6.78−6.82 (0.4H, m, *H*-3′), 6.85−6.90 (1.6H, m, *H*-3′), 7.08−7.12 (0.4H, m, *H*-2′), 7.17 (0.8H, dd, *J* = 7.5, 7.6 Hz, *H*-5), 7.26−7.29 (1.6H, m, *H*-2′), 7.31 (0.4H, d, *J* = 8.3 Hz), 7.38 (0.8H, dd, *J* = 7.6, 1.4 Hz, *H*-4), 7.74−7.80 (1H, m, *H*-6). ^{13}C NMR ($CDCl_3$, 125 MHz) δ 19.1, 21.6, 24.9, 43.5, 46.9, 55.4, 55.4, 83.8, 114.2, 114.3, 124.9, 127.3, 128.3, 129.1, 129.3, 129.4, 129.8, 130.3, 137.0, 137.3, 137.4, 141.8, 143.6, 159.2, 159.5, 170.6. HRMS $[M]^+$ ($C_{22}H_{28}BNO_4$) calcd 381.2220, obsd 381.2222.

*N,N-Bis(4-methoxybenzyl)-2-methyl-3-(4,4,5,5-tetramethyl-1,3,2-dioxaborolan-2-yl)benzenesulfonamide (**16**).* A mixture of **14** (0.18 mg, 0.41 mmol), bis(pinacolato)diboron (0.16 g, 0.62 mmol), [1,1′-bis(diphenylphosphino)ferrocene]dichloropalladium(II) (14 mg, 0.02 mmol), 1,1′-bis(diphenylphosphino)ferrocene (22 mg, 0.04 mmol), and KOAc (0.119 g, 1.21 mmol) in dioxane (2 mL) was purged under N_2 for 10 min and heated under microwave conditions 150 °C for 120 min. The cooled reaction mixture was filtered through Celite, diluted with EtOAc (10 mL), and washed with brine (3 × 10 mL). The combined organic fractions were dried ($MgSO_4$), and the solvent was remove under reduced pressure. Purification by chromatography on silica) using a gradient elution of petrol:EtOAc (10:1) from petrol:EtOAc (1:1) afforded the title compound as a white solid (87 mg, 40%); mp 126−128 °C. IR 2981, 2158, 1610, 1510 cm^{-1}. ^{1}H NMR ($CDCl_3$, 500 MHz) δ 1.38 (12H, s, CH_3), 2.79 (3H, s, Ar-CH_3), 3.79 (6H, s, OCH_3), 4.23 (4H, s, NCH_2), 6.76−6.81 (4H, m, *H*-3′), 6.92−6.98 (4H, m, *H*-2′), 7.28 (1H, dd, *J* = 7.8, 7.4 Hz, *H*-5), 7.95 (1H, dd, *J* = 7.4, 1.3 Hz, *H*-4), 8.07 (1H, dd, *J* = 7.8, 1.4 Hz, *H*-6). ^{13}C NMR ($CDCl_3$, 125 MHz): 19.1, 25.0, 48.6, 55.4, 84.1, 114.0, 125.2, 127.7, 130.2, 132.6, 139.0, 140.2, 144.6, 159.2. HRMS $[M]^+$ ($C_{29}H_{36}NO_6BS$) calcd 537.2465, obsd 537.2465.

6-Acylamino-2-amino-4-cyclohexylmethoxy-5-nitrosopyrimidines: Method I. General Procedure. To a solution of 2,6-diamino-4-cyclohexylmethoxy-5-nitrosopyrimidine[18] (**17**) (1.0 mol equiv) in DMF (5−10 mL) was added the appropriate anhydride (1.1 mol equiv), and the mixture was heated at 80 C° for the specified time. After cooling, volatiles were removed under reduced pressure, water (10−20 mL) was added, and the reaction mixture was extracted with EtOAc (3 × 20 mL). The combined organic fractions were dried (Na_2SO_4) and concentrated in vacuo, and the required acylaminopyrimidines (**18**−**23**) were isolated by chromatography on silica as described.

*6-Acetylamino-2-amino-4-cyclohexylmethoxy-5-nitrosopyrimidine (**18**).* Prepared from **17** (0.50 g, 2.0 mmol) and acetic anhydride (4 mL) in accordance with method I and purified by chromatography on silica (eluent DCM:MeOH, 10:1) to furnish **18** as an aquamarine crystalline solid (0.35 g; 60%); mp 149−150 °C. ^{1}H NMR (DMSO-d_6, 300 MHz) δ 1.13−1.29 (5H, m, cyclohexyl), 1.79−1.94 (6H, m, cyclohexyl), 2.57 (3H, s, Me), 4.45 (2H, d, *J* = 6.3, CH_2O), 8.73 (2 H, br s, NH_2), 12.3 (1 H, br s, NH). HRMS $[M]^+$ ($C_{13}H_{19}N_5O_3$) calcd 293.1488, obsd 293.1484. Anal. ($C_{13}H_{19}N_5O_3$ + 0.05 EtOAc) C, H, N.

*2-Amino-4-cyclohexylmethoxy-5-nitroso-6-propionylaminopyrimidine (**19**).* Synthesized from **17** (0.50 g, 2.0 mmol) and propionic anhydride (0.29 g, 2.2 mmol) in DMF (6.0 mL) following method I, purified by chromatography on silica employing petrol:EtOAc (3:2) as eluent, to give the title compound as an aquamarine crystalline solid (0.28 g, 46%); mp 160−161 °C. ^{1}H NMR (DMSO-d_6, 300 MHz) δ 1.11−1.18 (3H, t, *J* = 7.3 Hz, CH_2CH_3), 1.23−1.30 (5H, m, cyclohexyl), 1.78−1.94 (6H, m, cyclohexyl), 2.95 (2H, q, *J* = 7.3 Hz, CH_2CH_3), 4.44 (2H, d, *J* = 6.3 Hz, CH_2O), 8.72 (2H, br s, NH_2), 12.4 (1 H, br s, NH). HRMS $[M]^+$ ($C_{14}H_{21}N_5O_3$) calcd 307.1644, obsd 307.1632. Anal. ($C_{14}H_{21}N_5O_3$ + 0.3 EtOAc) C, H, N.

*2-Amino-4-cyclohexylmethoxy-6-isobutylamino-5-nitrosopyrimidine (**20**).* From **17** (0.82 g, 3.25 mmol) and isobutyric anhydride (0.57 g 3.57 mmol) in DMF (12 mL) employing method I, purification by chromatography on silica with petrol:EtOAc (3:2) as eluent, followed by recrystallization from EtOAc:petrol to furnish **20** as a pale-blue crystalline solid (0.63 g, 60%); mp 180−181 °C. ^{1}H NMR (DMSO-d_6, 300 MHz) δ 0.92−1.39 (5H, m, cyclohexyl), 1.22 (6H, d, *J* = 6.8 Hz, $CH(CH_3)_2$), 1.78−1.93 (6 H, m, cyclohexyl), 3.26 (1H, quin, *J* = 6.8 Hz, $CH(CH_3)_2$), 4.44 (2 H, d, *J* = 6.8 Hz, CH_2CH), 8.74 (2 H, br s, NH_2), 12.6 (1 H, br s, NH). Anal. ($C_{15}H_{23}N_5O_3$) C, H, N.

*2-Amino-6-benzoylamino-4-cyclohexylmethoxy-5-nitrosopyrimidine (**21**).* Synthesized following method I from **17** (0.50 g, 2.0 mmol) and benzoic anhydride (0.50 g; 2.2 mmol) in DMF (8 mL) and isolated by chromatography on silica using DCM:MeOH (95:5) as eluent. Recrystallization from EtOAc:petrol yielded **21** as a blue crystalline solid (0.24 g; 33.8%); mp 210−211 °C. ^{1}H NMR (DMSO-d_6, 300 MHz) δ 1.16−1.43 (5H, m, cyclohexyl), 1.81−1.98 (6 H, m, cyclohexyl), 4.50 (2H, d, *J* = 6.3 Hz, OCH_2), 7.75−7.86 (3H, m, Ar-H), 8.08−8.12 (2H, m, Ar-H), 8.88 (1 H, br s, NH), 8.99 (1H, br s, NH), 13.8 (1H, br s, NH). HRMS $[M]^+$ ($C_{18}H_{21}N_5O_3$) calcd 355.1644, obsd 355.1646. Anal. ($C_{18}H_{21}N_5O_3$) C, H, N.

*2-Amino-6-(2-chlorobenzoyl)amino-4-cyclohexylmethoxy-5-nitrosopyrimidine (**22**).* To a stirred solution of **17** (0.50 g, 2.00 mmol) and *N*,*N*-dimethyl-4-aminopyridine (24 mg, 0.20 mmol) in pyridine (12 mL) was added 2-chlorobenzoyl chloride (280 μL, 2.20 mmol). The solution was stirred at 25 °C under N_2 for 18 h and concentrated under reduced pressure, and the residual solid was dissolved in DCM (40 mL) and washed with aqueous hydrochloric acid solution (5% v/v, 3 × 20 mL). The organic fraction was dried (Na_2SO_4), and the solvent was removed in vacuo to give a dark-green solid, which was recrystallized from EtOAc:petrol to furnish the title compound as a blue−green crystalline solid (0.6 g; 78%); mp 184−185 °C. IR 3467, 3202, 2925, 1728, 1594, 1536 cm^{-1}. ^{1}H NMR (DMSO-d_6, 300 MHz) δ 0.94−1.28 (5H, m, cyclohexyl), 1.60−1.97 (6H, m, cyclohexyl), 4.35 (2H, d, *J* = 6.6 Hz, OCH_2), 6.15 (2H, s, NH_2), 7.32−7.53 (3H, m, Ar-H), 7.54 (1H, d, Ar-H). ^{13}C NMR, (DMSO-d_6, 75 MHz) δ 26.0, 26.7, 30.0, 37.5, 74.0, 127.7, 129.9, 131.3, 132.0, 132.8, 135.1, 139.6, 164.9, 166.6. MS (ES^+) *m*/*z* 390 $[M(^{35}Cl) + H]^+$, 392 $[M(^{37}Cl) + H]^+$. Anal. ($C_{18}H_{20}ClN_5O_3$ + 0.1 EtOAc) C, H, N.

*2-Amino-4-cyclohexylmethoxy-6-(2-methylbenzoyl)amino-5-nitrosopyrimidine (**23**).* Prepared analogously to **22** above from **17** (0.51 g, 2.00 mmol) and 2-methylbenzoyl chloride (300 μL, 2.20 mmol) in pyridine (12 mL). Recrystallization from EtOAc:petrol gave a dark-blue crystalline solid (0.57 g; 77%); mp 177−179 °C. IR 3418, 3233, 2916, 1713, 1598, 1520 cm^{-1}. ^{1}H NMR (DMSO-d_6, 300 MHz) δ 0.94−1.28 (5H, m, cyclohexyl), 1.60−1.95 (6H, m, cyclohexyl), 2.47 (3H, s, ArCH_3), 4.35 (2H, d, *J* = 6.7 Hz, OCH_2), 6.17 (1H, s), 7.22−7.57 (3 H, m, Ar−H), 7.57 (1H, s), 7.59 (1H, d, *J* = 1.2 Hz). ^{13}C NMR, (DMSO-d_6, 75 MHz) δ 21.0, 26.0, 26.7, 30.1, 37.5, 73.9, 126.8, 128.3, 132.2, 132.3, 134.5, 138.8, 139.8, 165.1, 168.9. MS (ES^+) *m*/*z* 370 $[M + H]^+$. Anal. ($C_{19}H_{23}N_5O_3$) C, H, N.

8-Substituted 2-Amino-6-cyclohexylmethoxypurines: Method II. General Procedure. A stirred solution of the appropriate 6-acylamino-2-amino-4-cyclohexylmethyloxy-5-nitrosopyrimidine (0.5−2.0 mmol) in THF (20−30 mL) containing AcOH (glacial, 1−2 mL) was cooled to −78 °C and purged with N_2 prior to addition of Pd (10% on carbon, 15% w/w). The reaction mixture was stirred under H_2 at atmospheric pressure for 24 h at ambient temperature and filtered through Celite, and the filtrate was neutralized with saturated $NaHCO_3$ solution (30−50 mL)

dx.doi.org/10.1021/jm401555v | *J. Med. Chem.* XXXX, XXX, XXX−XXX

and extracted with EtOAc (3 × 30 mL). The combined organic fractions were dried (Na_2SO_4) and evaporated under reduced pressure to give the required 8-substituted purine. Compound purification was achieved by chromatography on silica and recrystallization as described.

*2-Amino-6-cyclohexylmethoxy-8-methylpurine (**24**).* Prepared in accordance with method II from **18** (0.35 g, 1.20 mmol) and isolated by chromatography on silica employing DCM:MeOH (10:1) as eluent. Recrystallization from a mixture of EtOAc:MeOH gave **24** as a cream crystalline solid (0.19 g, 60%); mp 99−100 °C. ^{1}H NMR (DMSO-d_6, 300 MHz) δ 1.08−1.45 (5 H, m, cyclohexyl), 1.78−1.92 (6 H, m, cyclohexyl), 2.42 (3H, s, Me), 4.26 (2 H, d, J = 6.2 Hz, OCH_2), 6.20 (2 H, br s, NH_2), 12.2 (1 H, br s, NH). HRMS $[M]^+$ ($C_{13}H_{19}N_5O$) calcd 261.1590, obsd 261.1587. Anal. ($C_{13}H_{19}N_5O$ + 1.15 MeOH) C, H, N.

*2-Amino-6-cyclohexylmethoxy-8-ethylpurine (**25**).* Synthesized by method II from pyrimidine **19** (0.28 g, 0.91 mmol) and isolated by chromatography on silica employing petrol:EtOAc (3:2) as eluent. Recrystallization from a mixture of EtOAc:Et_2O gave **25** as a cream solid (0.10 g, 39.9%); mp 137−138 °C. ^{1}H NMR (DMSO-d_6, 300 MHz) δ 1.06−1.18 (5 H, m, cyclohexyl), 1.31 (3 H, t, J = 7.5 Hz, CH_2CH_3), 1.76−1.90 (6 H, m, cyclohexyl), 2.74 (2 H, q, J = 7.5 Hz, CH_2CH_3), 4.23 (2 H, d, J = 6.1 Hz, OCH_2), 6.18 (2 H, br s, NH_2), 12.2 (1 H, br s, NH). HRMS $[M]^+$ ($C_{14}H_{21}N_5O$) calcd 275.1746, obsd 275.1743. Anal. ($C_{14}H_{21}N_5O$ + 0.1 EtOAc) C, H, N.

*2-Amino-6-cyclohexylmethoxy-8-isopropylpurine (**26**).* In accordance with method II from **20** (0.63 g; 2.0 mmol). Isolated by chromatography on silica with DCM:MeOH (10:1) as eluent, followed by recrystallization from EtOAc:Et_2O to yield the title purine as a cream crystalline solid (0.39 g, 70%); mp 136−138 °C. ^{1}H NMR (DMSO-d_6, 300 MHz) δ 1.08−1.19 (5 H, m, cyclohexyl), 1.36 (6 H, d, J = 6.9 Hz, $CH(CH_3)_2$) 1.79−1.92 (6 H, m, cyclohexyl), 3.07 (1 H, quin, J = 6.9 Hz, $(CH(CH_3)_2)$, 4.25 (2 H, d, J = 6.1 Hz, OCH_2), 6.20 (2 H, br s, NH_2), 12.6 (1 H, s, NH). ($C_{15}H_{23}N_5O$ + 0.25 H_2O) C, H, N.

*2-Amino-6-cyclohexylmethoxy-8-phenylpurine (**27**).* Prepared following method II from **21** (0.24 g, 0.67 mmol) and isolated by chromatography on silica employing DCM:MeOH (10:1) as eluent. Recrystallization from MeOH:EtOAc gave **27** as pale-pink crystals (0.16 g, 76%); mp 271−272 °C. ^{1}H NMR (DMSO-d_6, 300 MHz) δ 1.12−1.31 (5H, m, cyclohexyl), 1.81−1.97 (6H, m, cyclohexyl), 4.33 (2H, d, J = 6.2 Hz, OCH_2), 6.43 (2H, br s, NH_2), 7.56−7.60 (3H, m, Ar-H), 8.16 (2 H, m, Ar-H), 13.0 (1H, br s, NH). HRMS $[M]^+$ ($C_{18}H_{21}N_5O$) calcd 323.1746, obsd 323.1746. ($C_{18}H_{21}N_5O$ + 0.4 MeOH) C, H, N.

*2-Amino-8-(2-chlorophenyl)-6-cyclohexylmethoxypurine (**28**).* Prepared from **22** (375 mg; 0.971 mmol) following method II and purified by chromatography on silica employing EtOAc:petrol (2:1), to afford the title compound as an off-white powder (241 mg, 70%); mp 190−191 °C. IR 3487, 3289, 3171, 2021, 1578 cm^{-1}. ^{1}H NMR (DMSO-d_6, 300 MHz) δ 1.02−1.33 (5H, m, cyclohexyl), 1.64−1.83 (6H, m, cyclohexyl), 4.23 (2H, d, J = 6.24 Hz, OCH_2), 6.34 (2H, br s, NH_2), 7.45−7.54 (2H, m, Ar-H), 7.61−7.64 (1H, m, Ar-H), 7.73−7.75 (1H, m, Ar-H), 12.69 (1 H, br s, NH). ^{13}C NMR, (DMSO-d_6, 75 MHz) δ 25.6, 26.4, 29.6, 37.2, 70.9, 114.7, 127.6, 130.4, 130.5, 131.3, 132.2, 145.1, 156.2, 160.2, 160.8. MS (ES$^+$) m/z 358 $[M(^{35}Cl) + H]^+$, 360 $[M(^{37}Cl) + H]^+$. Anal. ($C_{18}H_{20}ClN_5O$ + 0.1 EtOAc) C, H, N.

*2-Amino-6-cyclohexylmethoxy-8-(2-methylphenyl)purine (**29**).* Synthesized in accordance with method II from **23** (327 mg; 0.88 mmol) and purified by chromatography on silica with EtOAc:petrol (2:1); pale-yellow powder (302 mg, 100%); mp 187−188 °C. IR 3480, 3310, 3179, 3085, 2045, 1582 cm^{-1}. ^{1}H NMR (DMSO-d_6, 300 MHz) δ 1.01−1.29 (5H, m, cyclohexyl), 1.64−1.84 (6H, m, cyclohexyl), 2.54 (3H, s, Ar-CH_3), 4.25 (2H, d, J = 6.4 Hz, OCH_2), 6.28 (2H, br s, NH_2), 7.28−7.38 (3H, m, Ar-H), 7.64 (1H, m, Ar-H), 12.60 (1H, br s, NH). ^{13}C NMR (DMSO-d_6, 75 MHz) δ 21.3, 25.5, 26.3, 29.6, 37.2, 70.9, 114.9, 126.2, 129.3, 129.6, 130.3, 131.4, 137.6, 147.8, 156.3, 160.0, 160.6. MS (ES$^+$) m/z 338 $[M + H]^+$. HRMS $[M + H]^+$ ($C_{19}H_{24}N_5O$) calcd 338.1975, found 338.1973; $[M - H]^-$ ($C_{19}H_{22}N_5O$) calcd 336.1830, found 336.1826. Anal. ($C_{19}H_{23}N_5O$ + 0.2 EtOAc) C, H, N.

Purine **29** was also synthesized by the following alternative method: a mixture of 8-bromo-6-(cyclohexylmethoxy)-9*H*-purin-2-amine (83 mg; 0.25 mmol), *o*-tolyl boronic acid (69 mg; 0.51 mmol), Cs_2CO_3 (166 mg; 0.51 mmol), and dichloro [1,1′ bis(di-*tert*-butylphosphino)]ferrocene palladium(II) (8 mg; 0.01 mmol) in toluene (15 mL) was degassed with nitrogen and heated under at 100 °C with stirring for 3 h. After cooling, the reaction mixture was filtered through Celite and the filtrate was concentrated under reduced pressure to give a yellow solid. The crude material was purified by chromatography on silica, employing a gradient of petrol:EtOAc (1:1 to 0:1) as eluent to afford **29** as a beige−white solid (60 mg; 70%). All analytical data (mp, NMR, MS) were identical with **29** prepared previously.

*2,4,6-Triamino-5-cyclohexylmethoxypyrimidine (**30**).* Zinc powder (0.26 g, 3.9 mmol) was added to a solution of 2,6-diamino-4-cyclohexylmethoxy-5-nitrosopyrimidine (**17**, 0.20 g, 0.79 mmol) in AcOH (5 mL), and the solution was stirred for 12 h at room temperature. The reaction mixture was filtered through Celite, and the filtrate was evaporated under reduced pressure to furnish a yellow solid, which was redissolved in water (20 mL), and the solution was adjusted to pH 7.0 with saturated aqueous sodium bicarbonate solution. The mixture was extracted with EtOAc (3 × 30 mL), the combined organic layers were dried (Na_2SO_4), and the solvent was removed in vacuo to give a pale-yellow solid. Recrystallization from MeOH afforded the title compound (0.14 g, 74%); mp 151−153 °C. IR 3446, 3390, 3309, 3178, 2918, 2847, 1613, 1577 cm^{-1}. ^{1}H NMR (DMSO-d_6, 300 MHz) δ 0.92−1.29 (5H, m, cyclohexyl), 1.67−1.79 (6H, m, cyclohexyl), 3.39 (2H, br, NH_2), 3.93 (2H, d, J = 6.0 Hz, OCH_2), 5.27 (2H, br, NH_2), 5.66 (2H, br, NH_2). ^{13}C NMR, (DMSO-d_6, 75 MHz) δ 24.9, 25.7, 28.9, 36.7, 69.6, 99.9, 155.2, 155.4, 157.8. HRMS $[M]^+$ ($C_{11}H_{19}N_5O$) calcd 237.1587, obsd 237.1590. Anal. ($C_{11}H_{19}N_5O$ + 0.1 H_2O) C, H, N.

*2,5-Diamino-4-cyclohexylmethoxy-6-(2,2,2-trifluoroacetyl)-aminopyrimidine (**31**).* A solution of **30** (171 mg; 0.72 mmol) in TFA (5 mL) was heated under reflux for 6 h, and the solvent was evaporated in vacuo. The title compound was isolated as a yellow solid (213 mg; 91%) by chromatography on silica using DCM:MeOH, (9:1) as eluent and used directly for the next reaction. ^{1}H NMR (DMSO-d_6, 300 MHz) δ 0.95−1.17 (5H, m, cyclohexyl), 1.64−1.67 (6H, m, cyclohexyl), 3.98 (2H, d, J = 3.9, OCH_2), 6.98 (2H, br s, NH_2), 7.24 (2H, br s, NH_2), 9.97 (1H, s, NHCO). MS (ES$^+$) m/z 334 $[M + H]^+$.

*2-Amino-6-cyclohexylmethoxy-8-trifluoromethylpurine (**32**).* To a solution of **31** (213 mg; 0.64 mmol) in pyridine (6 mL) was added *N*,*N*-dimethyl-4-aminopyridine (21 mg; 0.17 mmol), and the mixture was heated under reflux for 5 days. The residual red oil remaining, following removal of the solvent under reduced pressure, was purified by chromatography on silica utilizing using DCM:MeOH (95:5) furnished the title compound as a pale-orange crystalline solid (106 mg; 53%); mp 252−253 °C. IR 3496, 1632, 1585 cm^{-1}. ^{1}H NMR (DMSO-d_6, 300 MHz) δ 0.97−1.32 (5 H, m, cyclohexyl), 1.63−1.81 (6 H, m, cyclohexyl), 4.23 (2H, d, J = 6.2 Hz, OCH_2), 6.76 (2H, br s, NH_2), 13.71 (1H, s, NH). ^{13}C NMR (DMSO-d_6, 75 MHz) δ 25.5, 26.3, 29.5, 37.1, 71.3, 114.2, 117.7, 121.3, 124.8, 155.3, 160.5, 161.9. MS (ES$^+$) m/z 316 $[M + H]^+$. Anal. ($C_{13}H_{16}F_3N_5O$ + 0.1 H_2O) C, H, N.

*2-Amino-9-benzyl-6-cyclohexylmethoxypurine (**33**).* To a solution of **5** (2.60 g, 10.5 mmol) in DMF (20 mL) was added K_2CO_3 (7.3 g, 52.6 mmol) and benzyl bromide (1.5 mL, 12.6 mmol), and the mixture was stirred at room temperature for 12 h. Volatiles were removed in vacuo, and the residual oil was redissolved in EtOAc (20 mL) and washed with water (3 × 25 mL), and the organic fraction was dried (Na_2SO_4) and evaporated under reduced pressure. Purification by chromatography on silica, using EtOAc:petrol (1:1) as eluent, gave the 9-benzylpurine (**33**) as a white solid (1.04 g, 29%). IR 3394, 3341, 3225, 3123, 2923, 2851, 1733, 1643, 1518 cm^{-1}. ^{1}H NMR (DMSO-d_6, 300 MHz) δ 0.95−1.27 (5H, m, cyclohexyl), 1.61−1.95 (6H, m, cyclohexyl), 4.21 (2H, d, J = 6.3 Hz, OCH_2), 5.25 (2H, s, CH_2Ph), 6.42 (2H, s, NH_2), 7.15−7.40 (5H, m, Ar−H), 7.95 (1H, s, purine C8−H). ^{13}C NMR (DMSO-d_6, 75 MHz) δ 26.1, 26.8, 30.2, 37.8, 47.2, 72.4, 116.0, 128.0, 128.5, 129.3, 136.4, 139.3, 154.7, 159.9, 162.3.

*9-Benzyl-8-(3-(benzyloxy)-2-methylphenyl)-6-(cyclohexylmethoxy)-9H-purin-2-amine (**34**).* 1-Benzyloxy-3-bromo-2-methylbenzene (616 mg, 2.22 mmol) and cesium carbonate (604 mg, 1.85 mmol) were added to a solution of **33** (250 mg, 0.74 mmol) in DMF (15 mL). The mixture was purged with N_2 for 15 min prior to addition of copper(I) iodide (423 mg, 2.22 mmol) and $Pd(OAc)_2$ (0.1 M in DMF, 0.37 mL) and heated for 40 min under microwave irradiation at 200 °C.

dx.doi.org/10.1021/jm401555v | J. Med. Chem. XXXX, XXX, XXX−XXX

The solvent was removed under reduced pressure, and the residual oil was redissolved in EtOAc (25 mL) and washed with water (3 × 25 mL) and dried (Na_2SO_4), and the organic fraction was evaporated in vacuo. The product was purified by chromatography on silica with petrol:AcOEt (2:1) as eluent to furnish the title compound as a pale-yellow solid (190 mg, 48%). IR: 3376, 3346, 3223, 2923, 2848, 1648, 1605, 1578 cm^{-1}. ^1H NMR ($CDCl_3$, 300 MHz) δ 0.95−1.15 (5H, m, cyclohexyl), 1.50−1.95 (6H, m, cyclohexyl), 1.85 (3H, s, Ar-CH_3), 4.23 (2H, d, J = 6.0 Hz, OCH_2), 4.84 (2H, br s, NH_2), 4.99 (2H, s, N-CH_2-Ar), 5.04 (2H, s, O-CH_2-Ar), 6.71−7.40 (13H, m, Ar-H). ^{13}C NMR ($CDCl_3$, 75 MHz) δ 13.5, 26.2, 26.9, 30.3, 37.9, 46.7, 70.9, 72.5, 113.8, 123.3, 126.6, 127.5, 127.9, 128.0, 128.2, 128.7, 128.9, 129.3, 131.9, 136.9, 137.7, 157.5, 159.7.

*Benzyl 3-(2-Amino-9-benzyl-6-(cyclohexylmethoxy)-9H-purin-8-yl)-2-methyl benzoate (**35**).* Synthesized in a manner analogous to that for **34** above from **33** (250 mg, 0.74 mmol) and benzyl 3-bromo-2-methylbenzoate (678 mg, 2.22 mmol). Purification by chromatography on silica with petrol:AcOEt (2:1) as eluent gave the title compound as a yellow powder (131 mg, 32%). IR 3349, 3225, 2923, 2851, 1721, 1653, 1603, 1580 cm^{-1}. ^1H NMR ($CDCl_3$, 300 MHz) δ 0.92−1.17 (5H, m, cyclohexyl), 1.55−1.97 (6H, m, cyclohexyl), 2.18 (3H, s, ArCH_3), 4.32 (2H, d, J = 6.0 Hz, OCH_2), 4.93 (2H, s, NH_2), 5.05 (2H, s, N-CH_2-Ar), 5.37 (2H, s, O-CH_2-Ar), 6.82−6.87 (2H, m, Ar-H), 7.10−7.50 (10H, m, Ar-H), 8.01 (1H, d, J = 7.5 Hz, Ar-H). ^{13}C NMR ($CDCl_3$, 75 MHz) δ 18.2, 26.1, 26.9, 30.3, 37.8, 46.7, 67.2, 72.5, 115.7, 125.6, 128.0, 128.5, 128.6, 128.8, 128.9, 131.8, 132.2, 132.6, 134.3, 136.4, 136.6, 140.6, 149.2, 155.6, 159.8, 162.1, 167.5.

*3-(2-Amino-6-cyclohexylmethoxy-9H-purin-8-yl)-2-methylphenol (**36**).* To a solution of **34** (125 mg, 0.23 mmol) in acetic acid (10 mL), containing hydrochloric acid (12M, 0.25 mL), was added Pd (10% on carbon, 125 mg), and the reaction mixture was stirred under H_2 at atmospheric pressure for 12 h. Water (10 mL) was added, and the mixture was heated under reflux for 1 h and filtered through Celite, and the solvents were evaporated under reduced pressure. Purification by semipreparative HPLC afforded the title compound as white crystals (11 mg, 13%). ^1H NMR (DMSO-d_6, 300 MHz) δ 0.99−1.84 (m, 11H, cyclohexyl), 2.17 (3H, s, Ar-CH_3), 4.21 (2H, d, J = 6.3 Hz, OCH_2), 6.80 (1H, d, J = 7.8 Hz, Ar-H), 6.90 (1H, d, J = 7.5 Hz, Ar-H), 6.99−7.05 (1H, dd, J = 7.8, 7.5 Hz, Ar-H), 8.43 (2H, br s, NH_2). HRMS $[M + H]^+$ ($C_{19}H_{24}N_5O_2$) calcd 354.1925, obsd 354.1925.

*3-(2-Amino-6-cyclohexylmethoxy-9H-purin-8-yl)-2-methylbenzoic Acid (**37**).* Prepared as described for **36** from **35** (105 mg, 0.19 mmol) and Pd (10% on carbon, 105 mg); purification by semipreparative HPLC gave the title compound as a white powder (17 mg, 24%). ^1H NMR DMSO-d_6, 300 MHz) δ 0.99−1.71 (m, 11H, cyclohexyl), 2.36 (3H, s, ArCH_3), 4.21 (2H, d, J = 6.3 Hz, CH_2), 7.15−7.20 (1H, m, Ar-H), 7.34 (1H, dd, J = 1.2, 7.5 Hz, Ar-H), 7.41 (1H, dd, J = 1.2, 7.5 Hz, Ar-H). ^{13}C NMR (DMSO-d_6, 75 MHz) 18.3, 27.3, 27.9, 31.0, 31.3, 39.3, 41.1, 73.3, 126.7, 129.9, 130.7, 132.6, 135.2, 142.8, 145, 150.0, 161.8. HRMS $[M + H]^+$ ($C_{20}H_{24}N_5O_3$) calcd 382.1874, obsd 382.1872.

*2-Amino-6-cyclohexylmethoxy-purine-9-carboxylic Acid t-Butyl Ester (**38**).* To a stirred suspension of **5** (98.4 mg; 4.0 mmol) and potassium carbonate (67.1 mg; 4.8 mmol) in DMF (12 mL) was added di-*t*-butyl dicarbonate (1.2 mL; 5.0 mmol), and the mixture was stirred at room temperature for 18 h. Water (20 mL) was added, and the reaction mixture was stirred a further 1 h, whereupon the resulting white precipitate was collected and triturated with Et_2O to give the product as a white solid (1.16 g; 84%); R_f = 0.61 (F). ^1H NMR ($CDCl_3$, 300 MHz) δ 1.01−1.32 (5 H, m, cyclohexyl), 1.68 (9H, s, $C(CH_3)_3$), 1.74−1.92 (6H, m, cyclohexyl), 4.28 (2H, d, J = 6.3 Hz, OCH_2), 5.14 (2H, br s, NH_2), 8.00 (1H, s, NH). ^{13}C NMR ($CDCl_3$, 75 MHz) δ 26.1, 26.8, 28.4, 30.1, 37.6, 72.5, 86.5, 137.7, 146.6, 153.9, 161.1, 162.3. HRMS $[M]^+$ ($C_{17}H_{25}N_5O_3$) calcd 347.1948, obsd 347.1957.

*2-Amino-8-bromo-6-cyclohexylmethoxypurine (**39**).* To a stirred suspension of **38** (1.13 g; 3.26 mmol) in MeCN (36 mL) and water (8.6 mL) was added *N*-bromosuccinimide (87.4 mg; 4.89 mmol). The mixture was stirred at room temperature for 1 h, filtered, and the filtrate concentrated under reduced pressure to give a tan solid. Purification by chromatography on silica using gradient elution with EtOAc:petrol (2:1) as eluent afforded the title compound as an off-white solid (442 mg, 41.6%); mp 228−229 °C. IR 3482, 3303, 3163, 2921, 2850, 1623, 1563 cm^{-1}. ^1H NMR ($CDCl_3$, 300 MHz) δ 1.04−1.31 (5H, m, cyclohexyl), 1.70−1.91 (6H, m, cyclohexyl), 4.28 (2H, d, J = 5.8 Hz, OCH_2), 5.10 (2 H, br s, NH_2). ^{13}C NMR ($CDCl_3$, 75 MHz): 26.1, 26.8, 30.1, 37.6, 72.8, 155.6, 158.8, 161.0. HRMS $[M]^+$ ($C_{12}H_{16}BrN_5O$) calcd 325.0536, obsd 325.0538.

Bromopurine **39** was also prepared directly from **5** as follows: A mixture of **5** (1.0 g; 4.0 mmol) and pyridinium tribromide (2.58 g; 8.1 mmol) in DCM (10 mL) was stirred at 70 °C for 96 h. Saturated aqueous sodium metabisulfite solution (10 mL) was added, followed by water (10 mL), and the mixture was extracted with EtOAc (3 × 20 mL). The organic phase was washed with brine (2 × 10 mL), dried ($MgSO_4$), and concentrated in vacuo. The residual solid was purified by chromatography on silica, employing EtOAc: MeOH (10:1) as eluent, to give **39** as an off-white solid (0.39 g; 29%), identical (mp, NMR, MS) to that prepared above.

*PMB-Protected 2-Amino-8-aryl-6-cyclohexylmethoxypurines (**40**−**42**): Method III. General Procedure.* A mixture of **39** (1.0 mol equiv), the appropriate benzamide (**15**) or sulfonamide (**16**) (1.0 mol equiv), dichloro [1,1′-bis(di-*tert*-butylphosphino)]ferrocene palladium-(II) ('Pd-118') (0.5 mol equiv), and Cs_2CO_3 (2.0 mol equiv) in dioxane:H_2O (4:1, 2.5 mL) was purged under N_2 for 15 min and stirred for 4 h at 110 °C. The reaction mixture was filtered through Celite, EtOAc (10 mL) was added, and the organic fraction was washed sequentially with saturated aqueous NH_4Cl and brine, dried over $MgSO_4$, filtered, and concentrated in vacuo. The target compound was isolated by chromatography on silica as described.

*3-(2-Amino-6-(cyclohexylmethoxy)-9H-purin-8-yl)-N-(4-methoxybenzyl)-2-methylbenzamide (**40**).* Prepared in accordance with method III from **39** (98 mg, 0.26 mmol) and **15** (84 mg, 0.26 mmol). Purification by chromatography on silica using a gradient eluent of 100% DCM to DCM:MeOH (5:1) afforded the title compound as a beige solid (54 mg; 42%); mp 252−255 °C. IR 3485, 3185, 2926, 1580, 1512 cm^{-1}. ^1H NMR (DMSO-d_6, 500 MHz) δ 0.98−1.09 (2H, m, cyclohexyl), 1.13−1.32 (3H, m, cyclohexyl), 1.62−1.75 (3H, m, cyclohexyl), 1.77−1.87 (3H, m, cyclohexyl), 2.43 (3H, s, Ar-CH_3), 3.74 (3H, s, OCH_3), 4.24 (2H, d, J = 6.4 Hz, OCH_2), 4.39 (2H, d, J = 6.0 Hz, NCH_2), 6.28 (2H, s, NH_2), 6.91 (2H, d, J = 8.7 Hz, *H*-3′), 7.28 (2H, d, J = 8.7 Hz, *H*-2′), 7.32−7.41 (2H, m, *H*-4, *H*-5), 7.61 (1H, br d, J = 7.0 Hz, *H*-6), 8.87 (1H, t, J = 6.0 Hz, N*H*), 12.63 (1H, s, N^9-*H*). ^{13}C NMR (DMSO-d_6, 125 MHz) δ 17.3, 25.2, 26.0, 29.3, 36.8, 41.8, 55.0, 70.6, 113.7, 125.5, 127.6, 128.5, 130.4, 131.5, 139.2, 158.2, 159.7, 168.9. HRMS $[M + H]^+$ ($C_{28}H_{33}N_6O_3$) calcd 501.2609, obsd 501.2598.

*3-(2-Amino-6-(cyclohexylmethoxy)-9H-purin-8-yl)-N,N-bis(4-methoxybenzyl)benzenesulfonamide (**41**).* Prepared following method III from 8-bromo-6-(cyclohexylmethoxy)-9*H*-purin-2-amine **39** (32 mg, 0.098 mmol), except that the diisopropyl (3-(*N*,*N*-bis(4-methoxybenzyl)sulfamoyl)phenyl)boronate was generated in situ as follows: To a solution of 3-bromo-*N*,*N*-bis(4-methoxybenzyl)-benzenesulfonamide **13** (62 mg, 0.13 mmol) in THF (2 mL) at −78 °C was added *n*-BuLi (2.5 M in hexane, 55 μL, 0.14 mmol) dropwise. The mixture was stirred for 10 min, triisopropylborate (35 μL, 0.15 mmol) was added, and stirring was continued for a further 15 min at −78 °C. The reaction mixture was allowed to warm to room temperature overnight, and the solvent was evaporated under reduced pressure to give diisopropyl (3-(*N*,*N*-bis(4-methoxybenzyl)sulfamoyl)phenyl)boronate (72 mg, 0.137 mmol), which was used directly. Purification by chromatography on silica, using a gradient elution from EtOAc:petrol (65:15) to 100% EtOAc, yielded the title compound as a white solid (18 mg; 29%). ^1H NMR ($CDCl_3$, 500 MHz) δ 0.91−1.05 (2H, m, cyclohexyl), 1.14−1.29 (3H, m, cyclohexyl), 1.63−1.87 (6H, m, cyclohexyl), 3.69 (6H, s, OCH_3), 4.03−4.23 (6H, m, NCH_2, OCH_2), 4.94 (2H, s, NH_2), 6.66 (4H, d, J = 8.1 Hz, *H*-3′), 6.85 (4H, d, J = 7.9 Hz, *H*-2′), 7.48 (1H, dd, J = 7.6, 7.9 Hz, *H*-3), 7.72 (1H, d, J = 7.6 Hz, *H*-4), 8.29 (1H, br s, *H*-6), 8.40 (1H, s, *H*-2). ^{13}C NMR ($CDCl_3$, 125 MHz) δ 25.8, 26.6, 29.9, 37.2, 49.8, 55.3, 72.3, 113. 9, 116.6, 124.6, 127.5, 127.8, 129.8, 129.9, 130.4, 131.1, 141.9, 146.6, 155.5, 159.2, 159.4, 161.7. HRMS $[M + H]^+$ ($C_{34}H_{39}N_6O_5S$) calcd 643.2697, obsd 643.2693.

*3-(2-Amino-6-(cyclohexylmethoxy)-9H-purin-8-yl)-N,N-bis(4-methoxybenzyl)-2-methylbenzenesulfonamide (**42**).* Prepared in accordance with method III from **39** (104 mg, 0.32 mmol) and **16** (171 mg, 0.32

dx.doi.org/10.1021/jm401555v | J. Med. Chem. XXXX, XXX, XXX−XXX

mmol). Purification by chromatography on silica with a gradient elution of 100% DCM to DCM:MeOH (10:1) gave the title compound as an-off white solid (24 mg; 24%); mp 209−210 °C. IR 3366, 2926, 1582, 1512 cm^{-1}. ^1H NMR (DMSO-d_6, 500 MHz) δ 0.99−1.11 (2H, m, cyclohexyl), 1.13−1.32 (3H, m, cyclohexyl), 1.63−1.76 (3H, m, cyclohexyl), 1.78−1.88 (3H, m, cyclohexyl), 2.63 (3H, s, Ar-CH_3), 3.72 (6H, s, OCH_3), 4.21−4.30 (6H, m, OCH_2, NCH_2), 6.35 (2H, s, NH_2), 6.84 (4H, d, J = 8.7 Hz, *H*-3′), 6.98 (4H, d, J = 8.7 Hz, *H*-2′), 7.50 (1H, dd, J = 7.3, 7.9 Hz, *H*-5), 7.84 (1H, d, J = 7.3 Hz, *H*-4), 7.95 (1H, d, J = 7.9 Hz, *H*-6), 12.76 (1H, s, N^9-*H*). ^{13}C NMR (DMSO-d_6, 125 MHz) δ 16.9, 25.2, 25.9, 29.3, 36.8, 48.9, 55.0, 70.6, 113.8, 114.5, 126.0, 127.3, 129.7, 129.9, 133.7, 134.6, 136.3, 139.6, 146.0, 155.9, 158.7, 159.8, 160.4. HRMS $[M + H]^+$ ($C_{35}H_{41}N_6O_5S$) calcd 657.2854, obsd 657.2840.

*2-Amino-8-aryl-6-cyclohexylmethoxypurines (**43**−**45**): Method IV. General Procedure.* A solution of the appropriate PMB-protected 2-amino-8-aryl-6-cyclohexymethyloxypurine (0.04−0.2 mmol) in TFA (1−2 mL) was stirred at the specified temperature until the reaction was complete. The reaction mixture was neutralized with saturated aqueous Na_2CO_3 solution and extracted with EtOAc (3 × 10 mL), and the combined organic fractions were dried ($MgSO_4$), filtered, and evaporated in vacuo. The target compounds were isolated by chromatography on silica as described.

*3-(2-Amino-6-(cyclohexylmethoxy)-9H-purin-8-yl)-2-methylbenzamide (**43**).* Synthesized from **40** (90 mg, 0.18 mmol) and TFA (1 mL) (48 h, 110 C) following method IV. Purification by chromatography on silica, using a gradient elution of 100% EtOAc to EtOAc:MeOH (5:1), gave the required purine as a white solid (4 mg; 6%); mp 271−272 °C. IR 3379, 3210, 2932, 2857, 1662, 1624, 1591, 1574, 1533 cm^{-1}. ^1H NMR (DMSO-d_6, 500 MHz) δ 1.02−0.14 (m, 2H, cyclohexyl), 1.16−1.36 (m, 3H, cyclohexyl), 1.65−1.79 (m, 3H, cyclohexyl), 1.80−1.92 (m, 3H, cyclohexyl), 2.52 (s, 3H, Ar-CH_3), 4.28 (d, 2H, J = 6.4 Hz, OCH_2), 6.32 (s, 2H, NH_2), 7.37 (dd, 1H, J = 7.4, 7.5 Hz, *H*-5), 7.43 (d, 1H, J = 7.4 Hz, *H*-4), 7.52 (s, 1H, N*H*), 7.63 (d, 1H, J = 7.5 Hz, *H*-6), 7.88 (s, 1H, N*H*), 12.67 (s, 1H, N*H*). ^{13}C NMR (DMSO-d_6, 125 MHz) δ 17.5, 26.8, 27.5, 30.8, 38.7, 72.8, 126.9, 129.5, 132.4, 132.6, 135.7, 139.7, 161.6, 175.2. HRMS $[M + H]^+$ ($C_{20}H_{25}N_6O_2$) calcd 381.2034, obsd 381.2030.

*3-(2-Amino-6-(cyclohexylmethoxy)-9H-purin-8-yl)-benzenesulfonamide (**44**).* In accordance with method IV from **41** (29 mg; 0.045 mmol) and TFA (1 mL) (3h at 20 °C). Purification by chromatography on silica, employing a gradient elution of EtOAc:petrol (4:1) to 100% EtOAc, furnished the title compound as a white solid (11 mg; 61%); mp 159−162 °C. IR 3323, 2920, 2851, 1651, 1625, 1530 cm^{-1}. ^1H NMR (MeOD-d_4, 500 MHz) δ 1.09−1.20 (2H, m, cyclohexyl), 1.24−1.40 (3H, m, cyclohexyl), 1.68−1.84 (3H, m, cyclohexyl), 1.90−1.97 (3H, m, cyclohexyl), 4.33 (2H, d, J = 6.2 Hz, OCH_2), 7.68 (1H, dd, J = 7.8, 7.9 Hz, *H*-5), 7.99 (1H, d, J = 7.8 Hz, *H*-4), 8.22 (1H, d, J = 7.9 Hz, *H*-6), 8.58 (1H, s, *H*-2). ^{13}C NMR (MeOD-d_4, 125 MHz) δ 26.9, 27.57,30.81, 38.78, 73.0, 125.21, 128.4, 130.75, 130.88, 131.8, 146.22, 161.61. HRMS $[M + H]^+$ ($C_{18}H_{23}N_6O_3S$) calcd 403.1547, obsd 403.1546.

*3-(2-Amino-6-(cyclohexylmethoxy)-9H-purin-8-yl)-2-methylbenzenesulfonamide (**45**).* Prepared in accordance with method IV from **42** (60 mg; 0.092 mmol) and TFA (1 mL) (90 min at 80 °C); isolated by chromatography on silica, using a gradient elution of 100% EtOAc to EtOAc:MeOH (5:1), to give the title compound as a white powder (30 mg; 78%); mp 258−259 °C. IR 3503, 3407, 2927, 2851, 1629, 1587 cm^{-1}. ^1H NMR (DMSO-d_6, 500 MHz) δ 0.94−1.10 (2H, m, cyclohexyl), 1.15−1.33 (3H, m, cyclohexyl), 1.61−1.75 (3H, m, cyclohexyl),1.77−1.86 (3H, m, cyclohexyl), 2.68 (3H, s, Ar-CH_3), 4.24 (2H, d, J = 6.3 Hz, OCH_2), 6.32 (2H, s, NH_2), 7.49 (1H, dd, J = 7.6, 7.8.Hz, *H*-5), 7.55 (2H, s, NH_2), 7.73 (1H, d, J = 7.6 Hz, *H*-4), 8.00 (1H, d, J = 7.8 Hz, *H*-6), 12.70 (1H, s, N*H*). ^{13}C NMR (DMSO-d_6, 125 MHz) δ 17.0, 25.2, 26.0, 29.2, 36.8, 70.6, 125.7, 143.4, 159.7, 160.3. HRMS $[M + H]^+$ ($C_{19}H_{25}N_6O_3S$) calcd 417.1703, obsd 417.1697.

Crystallography. Crystals of monomeric CDK2 (kindly supplied by C.A. Minshull, AstraZeneca, Macclesfield, UK) were soaked for 24 h in a 5 mM solution of compound **26** in mother liquor (50 mM ammonium acetate, 10% PEG-3350, 15 mM NaCl, 100 mM HEPES, pH = 7.4, 10% DMSO). The crystals were cryoprotected in 50 mM ammonium acetate, 10% PEG-3350, 25% glycerol, 100 mM HEPES, pH 7.4, and mounted into a 100 K nitrogen stream. Data collection was carried out at AstraZeneca, Macclesfield, UK, using a Bruker-Nonius FR591 rotating anode generator and an XrayResearch Mar345 image plate. Compounds **29**, **32**, **36**, **37**, **44**, and **45** were cocrystallized with CDK2/cyclin A as previously described.[20] Before data collection, crystals were briefly immersed in cryoprotectant (8 M sodium formate) before freezing.

Data processing was carried out using MOSFLM,[38] SCALA,[39] and other programs of the CCP4 suite.[40] The structures of CDK2/compound **26** and of compounds **29**, **32**, **36**, and **37** bound to CDK2/cyclin A were solved by molecular replacement using MOLREP[41] taking, respectively, the protein atoms of an unpublished structure of CDK2 bound to a derivative of **5** or CDK2/cyclin A/**7** (PDB accession code 1H1S[22]) as the search model. Structures of **44** and **45** bound to CDK2/cyclin A were solved by Phaser,[42] using as the search model a high-resolution structure of a recruitment peptide bound to CDK2/cyclin A (PDB accession code 2CCH). Each solution was then subjected to rigid body refinement in REFMAC,[43] revealing unambiguous electron density in the CDK2 ATP-binding site, consistent with the expected shapes of the inhibitors. Models of **26**, **29**, **32**, **36**, and **37** were created using the CCP4 Sketcher[40] and manually docked into the density using either O[43,44] (compounds **26** and **29**) or Coot[45] (compounds **32**, **36**, and **37**). Models of **44** and **45** were created using the Elbow Builder utility and built into the electron density using Coot. The inhibitor atoms were kept in all subsequent models during refinement. The structures were then refined further by rounds of manual rebuilding in O (for compounds **26** and **29**) or in Coot (compounds **32**, **36**, **37**, **44**, and **45**) and restrained refinement in REFMAC. Toward the end of refinement, waters were added using ARP/wARP[46] (compounds **26** and **29**) or the Coot water picking utility (**32**, **36**, **37**, **44**, and **45**) and manually verified. The statistics for the data sets and for the crystallographic refinement are presented in Supporting Information Table S1.

Modeling. The refined structure of mCDK2/compound **26** was aligned with CDK2/inhibitor structures using LSQKAB.[47] The kinases were aligned based on the α carbon positions of the residues Glu81, Phe82, Leu83, His84, Gln85, and Ala31. The hinge residues (Glu81−Gln85) were used as all the inhibitors investigated form hydrogen bonds with the backbone atoms in this region. Ala31 was used to allow the reliable alignment of the monomeric and the cyclin-bound CDK2 structures.[48]

Conformation-energy profiles were calculated with Gaussian.[47] Models were created using the CCP4 monomer sketcher[40] and InsightII (Accelrys, CA, USA) and then converted into *Z* matrices. The purine and aryl rings were constrained to coplanarity, and the models energy minimized with the 6-31G** basis set. Rigid potential energy scans were carried out at 5° intervals between the two coplanar conformations using the 3-21G basis set.

■ ASSOCIATED CONTENT

Ⓢ Supporting Information

Quantum mechanical calculations, structural data for the CDK2/cyclin A/17 and CDK2/cyclin A/18 complexes, and combustion analyses. This material is available free of charge via the Internet at http://pubs.acs.org.

Accession Codes

The structures of CDK2/compound **26**, and compounds **32**, **29**, **36**, **37**, **44**, and **45** bound to CDK2/cyclin A have been deposited in the PDB with accession codes 1W8C, 4CFN, 4CFM, 4CFV, 4CFU, 4CFX, and 4CFW, respectively.

■ AUTHOR INFORMATION

Corresponding Authors

*For J.A.E. (structural biology): phone, (44) 191 246 4422; fax, (44) 191 246 4301; E-mail, jane.endicott@ncl.ac.uk.

*For R.J.G. (medicinal chemistry): phone, (44) 191 222 8591; fax, (44) 191 222 8591; E-mail, r.j.griffin@ncl.ac.uk.

Present Addresses

#J.A.E. and M.E.M.N.: Northern Institute for Cancer Research, Newcastle University.

▽A.E.: Centre de Biochimie Structurale, Centre National de la Recherche Scientifique (CNRS), Institut National de la Santé et de la Recherche Médicale-Unités Mixtes de Recherche 5048 and 1054, Université Montpellier I, Montepellier, France.

Author Contributions

⊥These authors contributed equally to the work described in this paper.

Notes

The authors declare no competing financial interest.

■ ACKNOWLEDGMENTS

We would like to thank Julie Tucker and staff at AstraZeneca for providing facilities and for their assistance with data collection. We also thank beamline staff at the ESRF, Elettra, and The Diamond Light Source who provided excellent facilities for data collection. The authors would like to thank I. Taylor for technical support and T. Davies for useful discussions. This research was supported by grants from Cancer Research UK, Medical Research Council, and AstraZeneca.

■ ABBREVIATIONS USED

CDK, cyclin-dependent kinase; pRb, retinoblastoma protein; PI3-K, phosphatidylinositol-3-kinase; DMAP, 4-dimethylaminopyridine; PMB, 4-methoxybenzyl; HEPES, 4-(2-hydroxyethyl)-1-piperazineethanesulfonic acid

■ REFERENCES

(1) Malumbres, M.; Barbacid, M. Cell cycle, CDKs and cancer: a changing paradigm. *Nature Rev. Cancer* **2009**, *9*, 153−166.

(2) Lapenna, S.; Giordano, A. Cell cycle kinases as therapeutic targets for cancer. *Nature Rev. Drug Discovery* **2009**, *8*, 547−566.

(3) Romagosa, C.; Simonetti, S.; Lopez-Vicente, L.; Mazo, A.; Lleonart, M. E.; Castellvi, J.; Ramon, Y. C. S. p16(Ink4a) overexpression in cancer: a tumor suppressor gene associated with senescence and high-grade tumors. *Oncogene* **2011**, *30*, 2087−2097.

(4) Sherr, C. J.; Roberts, J. M. CDK inhibitors: positive and negative regulators of G1-phase progression. *Genes Dev.* **1999**, *13*, 1501−1512.

(5) Hunt, K. K.; Keyomarsi, K. Cyclin E as a prognostic and predictive marker in breast cancer. *Semin. Cancer Biol.* **2005**, *15*, 319−326.

(6) Wander, S. A.; Zhao, D.; Slingerland, J. M. p27: a barometer of signaling deregulation and potential predictor of response to targeted therapies. *Clin. Cancer Res.* **2011**, *17*, 12−18.

(7) Malumbres, M.; Pevarello, P.; Barbacid, M.; Bischoff, J. R. CDK inhibitors in cancer therapy: what is next? *Trends Pharmacol. Sci.* **2008**, *29*, 16−21.

(8) Hardcastle, I. R.; Golding, B. T.; Griffin, R. J. Designing inhibitors of cyclin-dependent kinases. *Annu. Rev. Pharmacol. Toxicol.* **2002**, *42*, 325−348.

(9) Bettayeb, K.; Tirado, O. M.; Marionneau-Lambot, S.; Ferandin, Y.; Lozach, O.; Morris, J. C.; Mateo-Lozano, S.; Drueckes, P.; Schachtele, C.; Kubbutat, M. H.; Liger, F.; Marquet, B.; Joseph, B.; Echalier, A.; Endicott, J. A.; Notario, V.; Meijer, L. Meriolins, a new class of cell death inducing kinase inhibitors with enhanced selectivity for cyclin-dependent kinases. *Cancer Res.* **2007**, *67*, 8325−8334.

(10) Sausville, E. Cell cycle regulatory kinase modulators: interim progress and issues. *Curr. Top. Med. Chem.* **2005**, *5*, 1109−1117.

(11) Galons, H.; Oumata, N.; Meijer, L. Cyclin-dependent kinase inhibitors: a survey of recent patent literature. *Expert Opin. Ther. Pat.* **2010**, *20*, 377−404.

(12) Tetsu, O.; McCormick, F. Proliferation of cancer cells despite CDK2 inhibition. *Cancer Cell* **2003**, *3*, 233−245.

(13) Ortega, S.; Presto, I.; Odajima, J.; Martín, A.; Dubus, P.; Sotillo, R.; Barbero, J. L.; Malumbres, M.; Barbacid, M. Cyclin-dependent kinase 2 is essential for meiotic but not for mitotic cell division in mice. *Nature Genet.* **2003**, *35*, 25−31.

(14) Berthet, C.; Aleem, E.; Coppola, V.; Tessarollo, L.; Kaldis, P. CDK2 knockout mice are viable. *Curr. Biol.* **2002**, *13*, 1175−1185.

(15) Molenaar, J. J.; Ebus, M. E.; Geerts, D.; Koster, J.; Lamers, F.; Valentijn, L. J; Westerhout, E. M.; Versteeg, R.; Caron, H. N. Inactivation of CDK2 is synthetically lethal to MYCN over-expressing cancer cells. *Proc. Natl. Acad. Sci. U. S. A.* **2009**, *106*, 12968−12973.

(16) Horiuchi, D.; Huskey, N. E.; Kusdra, L.; Wohlbold, L.; Merrick, K. A.; Zhang, C.; Creasman, K. J.; Shokat, K. M.; Fisher, R. P.; Goga, A. Chemical-genetic analysis of cyclin dependent kinase 2 function reveals an important role in cellular transformation by multiple oncogenic pathways. *Proc. Natl. Acad. Sci. U. S. A.* **2012**, *109*, E1019−E1027.

(17) Cheng, C. K.; Gustafson, W. C.; Charron, E.; Houseman, B. T.; Zunder, E.; Goga, A.; Gray, N. S.; Pollok, B.; Oakes, S. A.; James, C. D.; Shokat, K. M.; Weiss, W. A.; Fan, Q.-W. Dual blockade of lipid and cyclin-dependent kinases induces synthetic lethality in malignant glioma. *Proc. Natl. Acad. Sci. U. S. A.* **2012**, *109*, 12722−12727.

(18) Arris, C. E.; Boyle, F. T.; Calvert, A. H.; Curtin, N. J.; Endicott, J. A.; Garman, E. F.; Gibson, A. E.; Golding, B. T.; Grant, S.; Griffin, R. J.; Jewsbury, P.; Johnson, L. N.; Lawrie, A. M.; Newell, D. R.; Noble, M. E.; Sausville, E. A.; Schultz, R.; Yu, W. Identification of novel purine and pyrimidine cyclin-dependent kinase inhibitors with distinct molecular interactions and tumor cell growth inhibition profiles. *J. Med. Chem.* **2000**, *43*, 2797−2804.

(19) Gibson, A. E.; Arris, C. E.; Bentley, J.; Boyle, F. T.; Curtin, N. J.; Davies, T. G.; Endicott, J. A.; Golding, B. T.; Grant, S.; Griffin, R. J.; Jewsbury, P.; Johnson, L. N.; Mesguiche, V.; Newell, D. R.; Noble, M. E.; Tucker, J. A.; Whitfield, H. J. Probing the ATP ribose-binding domain of cyclin-dependent kinases 1 and 2 with O^6-substituted guanine derivatives. *J. Med. Chem.* **2002**, *45*, 3381−3393.

(20) Davies, T. G.; Bentley, J.; Arris, C. E.; Boyle, F. T.; Curtin, N. J.; Endicott, J.-A.; Gibson, A. E.; Golding, B. T.; Griffin, R. J.; Hardcastle, I. R.; Jewsbury, P.; Johnson, L. N.; Mesguiche, V.; Newell, D. R.; Noble, M. E. M.; Tucker, J. A.; Wang, L.; Whitfield, H.-J. Structure-based design of a potent purine-based cyclin-dependent kinase inhibitor. *Nature Struct. Biol.* **2002**, *9*, 745−749.

(21) Sayle, K. L.; Bentley, J.; Boyle, F. T.; Calvert, A. H.; Cheng, Y.; Curtin, N. J.; Endicott, J. A.; Golding, B. T.; Hardcastle, I. R.; Jewsbury, P.; Mesguiche, V.; Newell, D. R.; Noble, M. E.; Parsons, R. J.; Pratt, D. J.; Wang, L. Z.; Griffin, R. J. Structure-based design of 2-arylamino-4-cyclohexylmethyl-5-nitroso-6-aminopyrimidine inhibitors of cyclin-dependent kinases 1 and 2. *Bioorg. Med. Chem. Lett.* **2003**, *13*, 3079−3082.

(22) Hardcastle, I. R.; Arris, C. E.; Bentley, J.; Boyle, F. T.; Chen, Y.; Curtin, N. J.; Endicott, J. A.; Gibson, A. E.; Golding, B. T.; Griffin, R. J.; Jewsbury, P.; Menyerol, J.; Mesguiche, V.; Newell, D. R.; Noble, M. E.; Pratt, D. J.; Wang, L. Z.; Whitfield, H. J. N^2-Substituted O^6-cyclohexylmethylguanine derivatives: potent inhibitors of cyclin-dependent kinases 1 and 2. *J. Med. Chem.* **2004**, *47*, 3710−3722.

(23) Schulze-Gahmen, U.; Brandsen, J.; Jones, H. D.; Morgan, D. O.; Meijer, L.; Vesely, J.; Kim, S. H. Multiple modes of ligand recognition: crystal structures of cyclin-dependent protein kinase 2 in complex with ATP and two inhibitors, olomoucine and isopentenyladenine. *Proteins* **1995**, *22*, 378−391.

(24) Gray, N. S.; Wodicka, L.; Thunnissen, A. M.; Norman, T. C.; Kwon, S.; Espinoza, F. H.; Morgan, D. O.; Barnes, G.; LeClerc, S.; Meijer, L.; Kim, S. H.; Lockhart, D. J.; Schultz, P. G. Exploiting chemical libraries, structure, and genomics in the search for kinase inhibitors. *Science* **1998**, *281*, 533−538.

(25) Dreyer, M. K.; Borcherding, D. R.; Dumont, J. A.; Peet, N. P.; Tsay, J. T.; Wright, P. S.; Bitonti, A. J.; Shen, J.; Kim, S. H. Crystal structure of human cyclin-dependent kinase 2 in complex with the adenine-derived inhibitor H717. *J. Med. Chem.* **2001**, *44*, 524−530.

(26) Beattie, J. F.; Breault, G. A.; Ellston, R. P.; Green, S.; Jewsbury, P. J.; Midgley, C. J.; Naven, R. T.; Minshull, C. A.; Pauptit, R. A.; Tucker, J. A.; Pease, J. E. Cyclin-dependent kinase 4 inhibitors as a treatment for cancer. Part 1: Identification and optimization of substituted 4,6-bis anilino pyrimidines. *Bioorg. Med. Chem. Lett.* **2003**, *13*, 2955−2960.

(27) Breault, G. A.; Ellston, R. P.; Green, S.; James, S. R.; Jewsbury, P. J.; Midgley, C. J.; Pauptit, R. A.; Minshull, C. A.; Tucker, J. A.; Pease, J. E.

Cyclin-dependent kinase 4 inhibitors as a treatment for cancer. Part 2: Identification and optimization of substituted 2,4-bis anilino pyrimidines. *Bioorg. Med. Chem. Lett.* **2003**, *13*, 2961−2966.
(28) Thomas, H. D.; Wang, L.-Z.; Roche, C.; Bentley, J.; Cheng, Y.; Hardcastle, I. R.; Golding, B. T.; Griffin, R. J.; Curtin, N. J.; Newell, D. R. Preclinical in vitro and in vivo evaluation of the potent and specific cyclin-dependent kinase 2 inhibitor NU6102 and a water soluble prodrug NU6301. *Eur. J. Cancer* **2011**, *47*, 2052−2059.
(29) Fabbro, D.; Ruetz, S.; Buchdunger, E.; Cowan-Jacob, S.; Fendrich, G.; Liebetanz, J.; Mestan, J.; O'Reilly, T.; Traxler, P.; Chaudhuri, B.; Fretz, H.; Zimmermann, J.; Meyer, T.; Caravatti, G.; Furet, P.; Manley, P. Protein kinases as targets for anticancer agents: from inhibitors to useful drugs. *Pharmacol. Ther.* **2002**, *93*, 79.
(30) De-Azevedo, W. F.; Leclerc, S.; Meijer, L.; Havlicek, L.; Strnad, M.; Kim, S. H. Inhibition of cyclin-dependent kinases by purine analogues: crystal structure of human cdk2 complexed with roscovitine. *Eur. J. Biochem.* **1997**, *243*, 518−526.
(31) Legraverend, M.; Tunnah, P.; Noble, M.; Ducrot, P.; Ludwig, O.; Grierson, D. S.; Leost, M.; Meijer, L.; Endicott, J. Cyclin-dependent kinase inhibition by new C-2 alkynylated purine derivatives and molecular structure of a CDK2-inhibitor complex. *J. Med. Chem.* **2000**, *43*, 1282−1292.
(32) Schlosser, M.; Michel, D. About the "physiological size" of fluorine substituents: comparison of sensorially active compounds with fluorine and methyl substituted analogues. *Tetrahedron* **1996**, *52*, 99−108.
(33) Mettey, Y.; Gompel, M.; Thomas, V.; Garnier, M.; Leost, M.; Ceballos-Picot, I.; Noble, M.; Endicott, J.; Vierfond, J. M.; Meijer, L. Aloisines, a new family of CDK/GSK-3 inhibitors. SAR study, crystal structure in complex with CDK2, enzyme selectivity, and cellular effects. *J. Med. Chem.* **2003**, *46*, 222−236.
(34) Wang, S.; Meades, C.; Wood, G.; Osnowski, A.; Anderson, S.; Yuill, R.; Thomas, M.; Mezna, M.; Jackson, W.; Midgley, C.; Griffiths, G.; Fleming, I.; Green, S.; McNae, I.; Wu, S. Y.; McInnes, C.; Zheleva, D.; Walkinshaw, M. D.; Fischer, P. M. 2-Anilino-4-(thiazol-5-yl)pyrimidine CDK inhibitors: synthesis, SAR analysis, X-ray crystallography, and biological activity. *J. Med. Chem.* **2004**, *47*, 1662−1675.
(35) Brana, M. F.; Cacho, M.; Garcia, M. L.; Mayoral, E. P.; Lopez, B.; de Pascual-Teresa, B.; Ramos, A.; Acero, N.; Llinares, F.; Munoz-Mingarro, D.; Lozach, O.; Meijer, L. Pyrazolo[3,4-*c*]pyridazines as novel and selective inhibitors of cyclin-dependent kinases. *J. Med. Chem.* **2005**, *48*, 6843−6854.
(36) Galons, H.; Oumata, N.; Gloulou, O.; Meijer, L. Cyclin-dependent kinase inhibitors closer to market launch? *Expert Opin. Ther. Pat.* **2013**, *23*, 945−963.
(37) Guha, M. Cyclin-dependent kinase inhibitors move into Phase III. *Nature Rev. Drug. Discovery* **2012**, *11*, 892−894.
(38) Leslie, A. G. W. *Recent Changes to the MOSFLM Package for Processing Film and Image Plate Data*; Science and Engineering Research Council UK, Daresbury Laboratory, Warrington, UK, 1992, p 26.
(39) Evans, P. R. *Data Reduction*; Science and Engineering Research Council UK, Daresbury Laboratory: Warrington, UK, 1993; pp 114−122.
(40) CCP4. The CCP4 suite: programs for protein crystallography. *Acta Crystallogr., Sect. D: Biol. Crystallogr.* **1994**, *50*, 760−763.
(41) Vagin, A.; Teplyakov, A. MOLREP: an automated program for molecular replacement. *J. Appl. Crystallogr.* **1997**, *30*, 1022−1025.
(42) McCoy, A. J.; Grosse-Kunstleve, R. W.; Storoni, L. C.; Read, R. J. Likelihood-enhanced fast translation functions. *Acta Crystallogr., Sect. D: Biol. Crystallogr.* **2005**, *61*, 458−64.
(43) Murshudov, G. N.; Vagin, A. A.; Dodson, E. J. Refinement of macromolecular structures by the maximum-liklihood method. *Acta Crystallogr., Sect. D: Biol. Crystallogr.* **1997**, *53*, 240−255.
(44) Jones, T. A.; Zou, J. Y.; Cowan, S. W. Kjeldgaard. Improved methods for binding protein models in electron density maps and the location of errors in these models. *Acta Crystallogr., Sect. A: Found. Crystallogr.* **1991**, *47*, 110−119.
(45) Emsley, P.; Cowtan, K. Coot: model-building tools for molecular graphics. *Acta Crystallogr., Sect. D: Biol. Crystallogr.* **2004**, *60*, 2126−2132.
(46) Lamzin, V. S.; Wilson, K. S. Automated refinement of protein models. *Acta Crystallogr., Sect. D: Biol. Crystallogr.* **1993**, *49*, 129−147.
(47) Frisch, M. J.; Trucks, G. W.; Schlegel, H. B.; Scuseria, G. E.; Robb, M. A.; Cheeseman, J. R.; Zakrzewski, V. G.; Montgomery, J. A., Jr.; Stratmann, R. E.; Burant, J. C.; Dapprich, S.; Millam, J. M.; Daniels, A. D.; Kudin, K. N.; Strain, M. C.; Farkas, O.; Tomasi, J.; Barone, V.; Cossi, M.; Cammi, R.; Mennucci, B.; Pomelli, C.; Adamo, C.; Clifford, S.; Ochterski, J.; Petersson, G. A.; Ayala, P. Y.; Cui, Q.; Morokuma, K.; Malick, D. K.; Rabuck, A. D.; Raghavachari, K.; Foresman, J. B.; Cioslowski, J.; Ortiz, J. V.; Baboul, A. G.; Stefanov, B. B.; Liu, G.; Liashenko, A.; Piskorz, P.; Komaromi, I.; Gomperts, R.; Martin, R. L.; Fox, D. J.; Keith, T.; Al-Laham, M. A.; Peng, C. Y.; Nanayakkara, A.; Gonzalez, C.; Challacombe, M.; Gill, P. M. W.; Bohnson, B.; Chen, W.; Wong, M. W.; Andres, J. L.; Gonzalez, C.; Head-Gordon, M.; Replogle, E. S.; Pople, J. A. *Gaussian 1998*, version A.7; Gaussian, Inc.: Pittsburgh, PA, 1998.
(48) Davies, T. G.; Tunnah, P.; Meijer, L.; Marko, D.; Eisenbrand, G.; Endicott, J. A.; Noble, M. E. Inhibitor binding to active and inactive CDK2: the crystal structure of CDK2-cyclin A/indirubin-5-sulphonate. *Structure (Cambridge, MA, U. S.)* **2001**, *9*, 389−397.